Elsevier Editorial System(tm) for European Polymer Journal

Manuscript Draft

Manuscript Number: EUROPOL-D-15-01323

Title: Poly(butylene succinate)-based composites containing □-cyclodextrin/D-limonene inclusion complex

Article Type: Research Paper

Section/Category: Regular Paper

Keywords: Poly(butylene succinate), β-cyclodextrin, D-limonene, Biocomposites, Thermal stabilization

Corresponding Author: Dr. Gabriella Santagata,

Corresponding Author's Institution: Institute for Polymers, Composites and Biomaterials, National Council of Research

First Author: Salvatore Mallardo

Order of Authors: Salvatore Mallardo; Valentina De Vito; Mario Malinconico; Maria Grazia Volpe; Gabriella Santagata; Maria Laura Di Lorenzo

Abstract: Structural, morphological and thermal properties of films based on poly(butylene succinate) (PBS) and inclusion complex of beta-cyclodextrins (beta-CD) and D-limonene were studied, in order to prepare novel bio-active food packaging materials. The inclusion complex contains 7 wt% of D-limonene, as quantified by precipitation, as well as by thermogravimetry. Inclusion within beta-CD cavity stabilizes D-limonene against evaporation, even upon melt compounding with PBS. Infrared spectroscopy, performed on compression molded films, evidenced both the D-limonene encapsulation inside beta-CD cages, and the occurrence of hydrogen bonding between hydroxyl groups of beta-CD-lim complex and ester units of PBS. Optical micrographs showed a phase separated morphology even if, the existence of physical interactions between the polar groups allowed a homogeneous and fine distribution of particles within polymeric matrix. DSC analysis highlighted the anti-nucleating action of beta-CD-lim complex towards PBS, evidenced by a strong delay in kinetics of PBS crystallization process.

Suggested Reviewers: Veronica Ambrogi
ambrogi@unina.it
biodegradable and biobased polymers for food packaging application

Maria Amparo Chiralt Boix
dchiralt@tal.upv.es
She is expert in polymeric based systems for food packaging materials and their chemical-physical characterization

Yves Grohens
yves.grohens@univ-ubs.fr
biodegradable polymers, polymer composites

Pawel Sajkiewicz
psajk@ippt.pan.pl
biodegradable semicrystalline polymers, crystallization kinetics

Sarai Agustin-Salazar
iq.saraiasalazar@gmail.com
natural bioactive molecules, biopolymers, packaging

European Polymer Journal
Editorial Office
Prof. A.J. Müller
University of the Basque Country, Donostia-San Sebastián, Spain

Dear Prof. A.J. Müller,

we wish you to consider our manuscript entitled "Poly(butylene succinate)-based composites containing β-cyclodextrin/D-limonene inclusion complex" by Salvatore Mallardo, Valentina De Vito, Mario Malinconico, Maria Grazia Volpe, Gabriella Santagata, Maria Laura Di Lorenzo for publication in one of the forthcoming issues of European Polymer Journal.

This paper is the result of a novel approach finalized to investigate the chemical-physical properties of biocomposites based on Poly(butylene succinate) and inclusion complex (IC) of D-limonene within β-cyclodextrin, in order to obtain new biodegradable films, potentially exploitable as bioactive food packaging materials. Particular attention is given to interactions occurring between the polar groups of inclusion complex and ester units of polymeric matrix, as well as to the influence of the IC on structural and thermal properties of PBS.

Since the paper is focused on the study of physical-chemical properties of PBS based biocomposites, all the authors mutually agree that this manuscript should be submitted to European Polymer Journal, due to its wide interest in the physics and chemistry of polymers.

I confirm that the manuscript describes original research not submitted for publication or already published elsewhere.

We thank You in advance for considering our work, and look forward to hearing from you soon.

Kind Regards,

Gabriella Santagata,

On behalf of the co-authors.

Any communication should be sent to:
Dr. Gabriella Santagata
Institute for Polymers, Composites and Biomaterials, CNR
Via Campi Flegrei 34, Comprensorio Olivetti,
80078 Pozzuoli (Napoli), Italy
Tel: +39 081 8675214
fax: +39 081 8675230
E-mail: santagata@ipcb.cnr.it

*Graphical Abstract

Poly(butylene succinate)-based composites containing β-cyclodextrin/D-limonene inclusion complex

Salvatore Mallardo[1], Valentina De Vito[2], Mario Malinconico[1], Maria Grazia Volpe[2], Gabriella Santagata[1], Maria Laura Di Lorenzo[1]

[1]*Institute for Polymers, Composites and Biomaterials: National Council of Research, via Campi Flegrei 34, 80078 Pozzuoli, Naples, Italy*

[2]*Institute of Food Science, National Council of Research Via Roma, 64 83100 Avellino Italy*

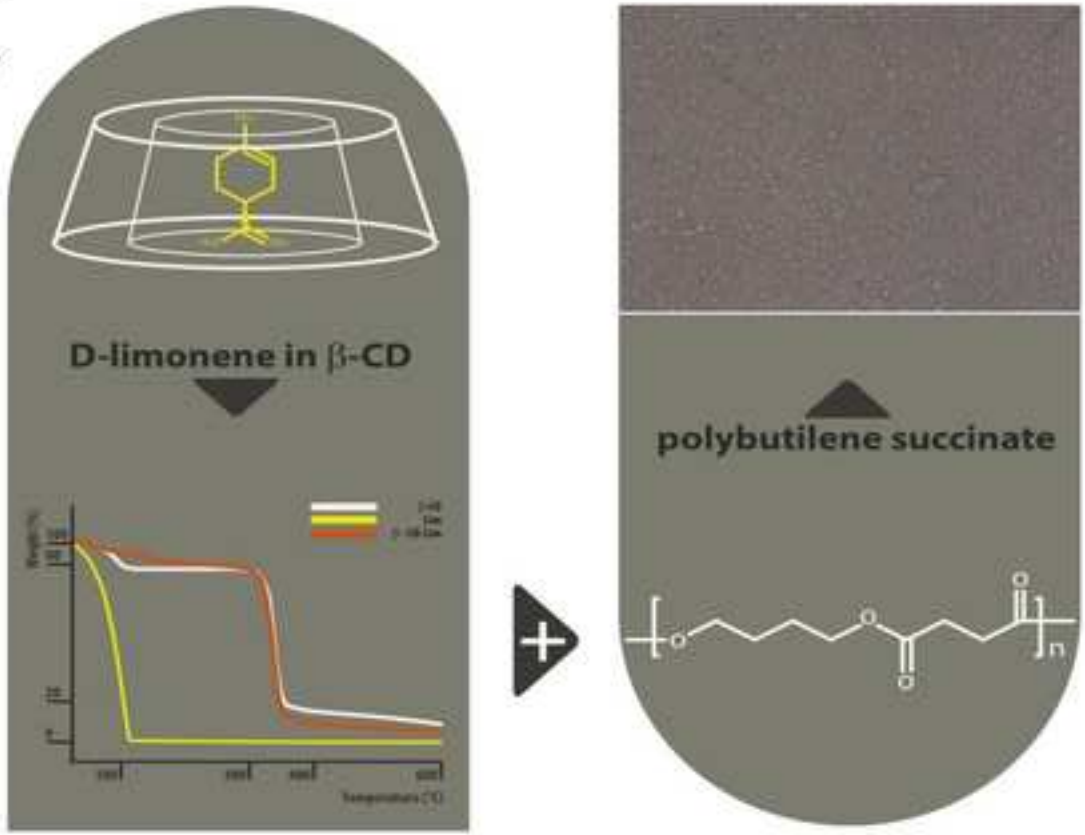

Highlights

1) Inclusion complex (IC) of D-limonene inside β-cyclodextrins (β-CD) cages was prepared.

2) Poly(butylene succinate) (PBS) and IC composites were prepared by melt extrusion.

3) Homogeneous dispersion of IC in PBS was proven by optical microscopy and infrared spectroscopy

4) D-limonene was thermally stabilized upon inclusion within β-CD cages as shown by TGA analysis

5) IC delays melt crystallization of PBS as shown by isothermal and non-isothermal DSC analysis.

Poly(butylene succinate)-based composites containing β-cyclodextrin/D-limonene inclusion complex

Salvatore Mallardo[1], Valentina De Vito[2], Mario Malinconico[1], Maria Grazia Volpe[2], Gabriella Santagata[1*], Maria Laura Di Lorenzo[1*]

[1]Institute for Polymers, Composites and Biomaterials; National Council of Research, via Campi Flegrei 34, 80078 Pozzuoli, Naples, Italy

[2]Institute of Food Science, National Council of Research
Via Roma, 64 - 83100 Avellino - Italy

Abstract

Structural, morphological and thermal properties of films based on poly(butylene succinate) (PBS) and inclusion complex of β-cyclodextrins (β-CD) and D-limonene were studied, in order to prepare novel bio-active food packaging materials. The inclusion complex contains 7 wt% of D-limonene, as quantified by precipitation, as well as by thermogravimetry. Inclusion within β-CD cavity stabilizes D-limonene against evaporation, even upon melt compounding with PBS. Infrared spectroscopy, performed on compression molded films, evidenced both the D-limonene encapsulation inside β-CD cages, and the occurrence of hydrogen bonding between hydroxyl groups of β-CD-lim complex and ester units of PBS. Optical micrographs showed a phase separated morphology even if, the existence of physical interactions between the polar groups allowed a homogeneous and fine distribution of particles within polymeric matrix. DSC analysis highlighted the anti-nucleating action of β-CD-lim complex towards PBS, evidenced by a strong delay in kinetics of PBS crystallization process.

Keywords: Poly(butylene succinate), β-cyclodextrin, D-limonene, biocomposites, Thermal stabilization

Introduction

* Corresponding author. Email: gabriella.santagata@ipcb.cnr.it
* Corresponding author. Email: dilorenzo@ipcb.cnr.it

Cyclodextrins (CD) comprise a family of cyclic oligosaccharides produced from a renewable natural material, starch, by enzymatic conversion [1]. The three major cyclodextrins are crystalline and appear as torus-like macro-rings built up from glucopyranose units. The α-cyclodextrin comprises six glucopyranose units, β-CD is made of seven units, and γ-CD comprises eight units [1].

The cyclodextrins are well known for being biocompatible, biodegradable, and soluble in water. In an aqueous solution, the slightly apolar cyclodextrin cavity is occupied by water molecules, which are energetically unfavored (polar-apolar interaction), and therefore can be readily substituted by appropriate "guest molecules" that are less polar than water. The formed inclusion complex (IC) can be isolated as a stable crystalline material [1]. The ability to include small molecules within their cavity led to large development of CDs for a number of applications in the pharmaceutical, food, cosmetic industry. The diffusivity and volatility (in case of volatile molecules) of the included guest decrease strongly, and the guest is protected from oxidation, thermal decomposition, etc. when inserted within the host cavity.

Cyclodextrins are also used to prepare inclusions complexes with linear aliphatic polymers [2]. The guest polymer chains occupy narrow cylindrical channels, with diameter of 5-10 Å, created by the crystalline CD host lattice [3]. As a consequence, the included polymer chains are constrained to assume highly extended conformations and are generally segregated from neighboring included polymer chains by the channel walls of the host crystalline CD lattice. In other words, polymer-CD ICs can generate new materials with peculiar morphologies and specific thermal, mechanical, and barrier properties. The formation and properties of ICs of CDs with various polymers have been studied, to improve polymer miscibility [4] biodegradation [5] and crystallization [6]. A number of biodegradable polyesters were specifically investigated, like poly(lactic acid) [3, 7-8], poly(hydroxyalcanoates) [9, 10], poly(ε-caprolactone) [2,3, 11, 12], poly(butylene succinate) [2, 12], etc. since the CDs can act as biodegradable and biocompatible additives when exploited to form inclusion complexes with linear polymers.

Conversely, only limited research was conducted by incorporating CDs as filler in polymer composites. More specifically, CDs can be used to include small molecules within their cavity, with limited interactions with the polymer chain. In the research detailed below, β-cyclodextrin was used as cage to include D-limonene (4-isopropenyl-1-methylcyclohexene), the major constituent in several citrus-derived essential oils (e.g. orange, lemon, mandarin, lime, grapefruit, etc.), which is also a natural antimicrobial agent [13-15]. Although traditional chemical preservatives and synthetic antimicrobials are commonly used to prevent growth of food borne and spoilage microorganisms, recent investigations evidenced that these additives are responsible of adverse reactions in humans,

producing toxic substances and carcinogens [16-18]. As a matter of fact, natural antimicrobial substances, like D-limonene, may be regarded as valid safe alternatives that could achieve comparable or improved preservative effects.

D-limonene is listed in the Code of Federal Regulations and generally recognized as safe flavoring agent and food preservative [19]. Its outstanding antimicrobial activities have already been tested with different species of food-related microorganisms, such as Staphylococcus aureus, Listeria monocytogenes, Salmonella enterica, Saccharomyces bayanus and more [20-21]. Unfortunately, D-limonene is susceptible to oxidative degradation, which directly results in its loss of activity [19,22]. Moreover, similar to other volatile essential oils, limonene aroma could be easily released to the packaged food, thus contaminating it. In order to overcome to these drawbacks, D-limonene was included into CDs, and the inclusion complex CD-lim thus obtained was dispersed into a biodegradable and biobased polymer matrix, namely poly(butylene succinate) (PBS).

PBS is a biodegradable and biobased polyester, synthesized via polycondensation of succinic acid (or dimethyl succinate) and 1,4-butanediol, i.e. from monomers that can be derived from fossil-based or renewable resources. PBS is currently used for food packaging, and its use in this market area is expected to largely increase in the coming years [23]. The aim of this paper is to investigate the chemical-physical properties of biodegradable PBS biobased films containing an inclusion complex of β-cyclodextrins and D-limonene. Particular attention is given to interactions between the polymeric matrix and IC, and to the influence of the inclusion complex on structural and thermal properties of PBS, with the aim to develop novel bio-active food packaging materials.

Experimental Part

Materials

Poly(butylene succinate) (PBS) (GS Pla®,Grade AZ71TN,) with MFI of 220 g/10 min (155°C, 2.16 kg) was purchased from Mitsubishi Chemicals Corporation (Tokio, Japan).

β-cyclodextrin (CD), provided by Sigma-Aldrich, was used after drying; D-limonene (90% purity), kindly supplied by Diego Visalli s.r.l., was used as raw material in the microencapsulation process.

Preparation of CD-lim inclusion complex

A precipitation method was used to obtain β-cyclodextrins/limonene complex (CD-lim) [24-25]. 50 g of CD were dissolved in 500 mL of an ethanol/water (1:2) mixture at 55 °C. D-limonene was first dissolved in ethanol (10% w/v), then slowly added to the warm CD solution under continuous stirring. The obtained mixture was covered and further stirred for additional 4 h at room

temperature, then stored overnight at 4 °C. The precipitated CD-lim complex was recovered by filtration and dried at 50 °C for 24 h, and at 25 °C for additional 24 h. CD-lim powder was stored at 25 °C in an airtight bottle. The estimated final percentage of limonene included in β-CD was 7% w/w.

Composites preparation

PBS pellets were dried at 60 °C overnight in vacuum oven prior to extrusion. PBS/CD-lim systems containing up to 20 wt% of CD-lim, were prepared by melt mixing in a HAAKE MiniLAb extruder equipped with anti-rotating twin-screw with length of 150 mm. Extrusion was performed at 135 °C, for 3 minutes at screws rotation speed of 40 rpm. Binary composites of PBS/CD-lim were prepared and, from now on, coded as weight/weight ratio: 100/0, 90/10, 80/20.

Preparation of Compression-Molded Sheets

PBS/CD-lim systems were dried at 60°C overnight in vacuum oven, then compression-molded using a compression molding press (Model C, Carver Laboratory Press, USA), in order to prepare films. About 2 g of pellets were placed between two steel plates, pre-heated at 130 °C for 2 min at 220 KPa and compression molded for 4 minutes by rising the pressure up to 870 KPa; the samples were then cooled to room temperature by means of cold water circulating in the plates of the press.

Fourier Transform Infrared (FTIR-ATR) spectroscopy

Attenuated Total Reflection Fourier Transform Infrared (FTIR-ATR) spectroscopy was carried out on the surface of PBS/CD-lim compression molded films, as well as on β-CD and CD-lim powders, by means of a Perkin-Elmer Spectrum 100 spectrometer, equipped with a Universal ATR diamond crystal sampling accessory. All the samples were analysed at room temperature. Spectra were recorded as an average of 64 scans in the range 4000–480 cm^{-1}, with a resolution of 4 cm^{-1}. No mathematical correction (e.g. smoothing) was done, and spectroscopic manipulation, such as baseline adjustment and normalization, were performed using the Spectracalc software package OMNIC 9 (Thermo Fisher Scientific, Inc., MA, USA). Before testing, all samples were dried in oven at 60°C for 24 hours.

Thermogravimentric Analysis (TGA)

Thermogravimetric analyses (TGA) were carried out with a Mettler Thermogravimetric Analyzer Mod. TG 50. Measurements were performed on samples of about 8–10 mg, placed in open ceramic crucibles and heated from room temperature to 600 ºC at 20 ºC/min in nitrogen atmosphere, with a

nominal gas flow rate of 30 mL/min. Before the tests, a blank curve was measured and subtracted from the single thermograms, to correct from instrumental drift [26].

Optical microscopy

Morphology of PBS/CD-lim films was analyzed by optical microscopy, using a Zeiss polarizing microscope equipped with a Linkam TMHS 600 hot stage. A small piece of each film was squeezed between two microscope slides, then inserted in the hot stage. Photomicrographs were taken with a Scion Corporation CFW-1312C Digital Camera and recorded using the software Image-Pro Plus 7.0. Dry nitrogen gas was purged throughout the hot stage during analyses.

Differential Scanning Calorimetry (DSC)

The thermal properties of PBS/CD-lim based systems were investigated using a Q2000 Tzero differential scanning calorimeter (DSC), TA Instrument, equipped with a RCS cooling accessory. The calorimeter was calibrated in temperature and energy with indium. Dry nitrogen was used as purge gas at a rate of 50 ml/min.

Each compression-molded PBS/CD-lim sample was heated from 25 to 135 °C at a rate of 20 °C/min, melted at 135 °C for 2 minutes to erase previous thermal history, quickly cooled to the desired isothermal crystallization temperature (T_c), maintained at T_c until completion of the phase transition, then heated to 150 °C at 20 °C/min.

Non-isothermal crystallization experiments were performed by quickly cooling the compression-molded sheets to 120° C after melting at 135 °C for 2 min, followed by cooling at various rates, ranging from 0.5, 1, 2 to 4 °C/min. Crystallization is an exothermic process, and the heat evolved during the phase transition may cause local heating and thermal gradients within the sample. As a consequence, transitions can occur at temperatures that do not correspond to those detected by the instrumentation [26-27]. The thicker the sample, the more critical this problem is. Therefore, for non-isothermal analyses sample mass was limited to 3.0 ± 0.2 mg, and cooling rates not exceeding 4 °C/min were used.

Before DSC measurements, the samples were dried under vacuum at room temperature for 24h. A fresh specimen was used for each analysis. All the experiments were repeated three times to ensure reproducibility.

Results and Discussion

The effective content of D-limonene included within β-CD cavity or absorbed on its surface was determined following the procedure described in Ref. [25]. Comparison of the initial weight of β-cyclodextrin, with the mass of the material after complex formation and the subsequent drying process, revealed that the CD-lim complex contains 7 wt% of D-limonene. Extraction with *n*-hexane showed that only a minor amount of limonene was absorbed on β-CD external surface, being instead caged into β-CD cavity.

Inclusion of limonene inside β-CD hollow was also confirmed by infrared spectroscopy (FTIR) analysis, which can provide indication related to guest and host molecules association. In Figure 1 the FTIR-ATR spectra of neat β-CD, CD-lim complex and their difference spectrum are reported.

β-CD spectrum, presented in Figure 1-a, shows a very strong broad band centred at 3297 cm^{-1} ascribed to -OH stretching vibrational modes coming from both primary and secondary -OH groups bonded intra- or inter-molecularly, and interstitial and intra-cavity water molecules [28]. -OH scissoring vibration occurs at 1414 cm^{-1}, whereas out-of-plane bending vibrations appear at 605, 577, 527 cm^{-1}. Stretching vibration of CH_2 and CH are evidenced at 2926 cm^{-1}, while their scissoring vibrations are observed at 1365, 1330 and 1254 cm^{-1}. C-O-C symmetric and asymmetric vibrations appear at 1152, 997 and 947 cm^{-1}, and C-O stretching vibration occur at 1076 and 1021 cm^{-1} [29]. Another characteristic broad peak observable at about 1643 cm^{-1}, concerns the vibration modes of different types of water molecules located inside β-CD cavities [30].

All the characteristic FT-ATR absorption peaks of β-CD can be detected also in CD-lim complex spectrum (Figure 1-b). Actually, curve profiles are very similar, since most of the vibration frequencies typical of limonene functional groups are overlapped by prominent β-CD absorption peaks.

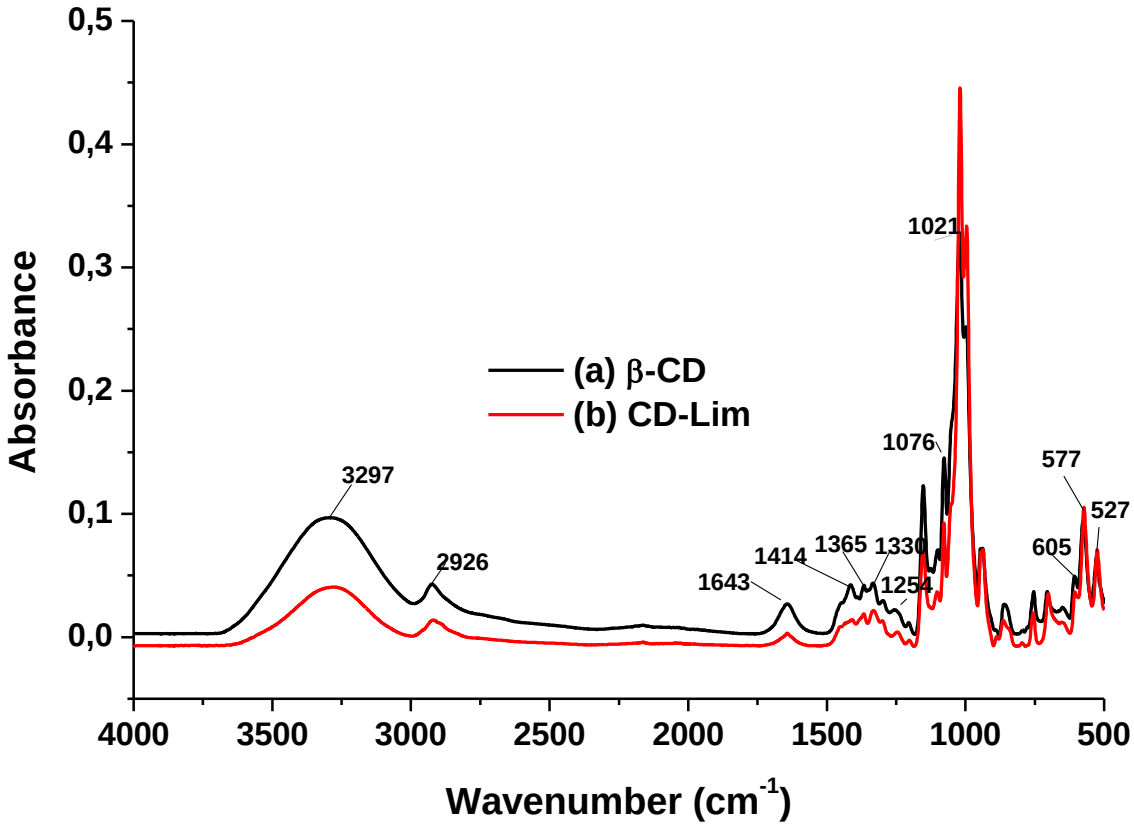

Fig 1 (a,b). FTIR-ATR spectra of: (a) β-CD, and (b) CD-Lim inclusion complex

In order to evidence the adsorption bands of limonene and to emphasize formation of CD-lim inclusion complex, a spectral subtraction between CD-lim and β-CD samples was performed and reported in Figure 1-c.

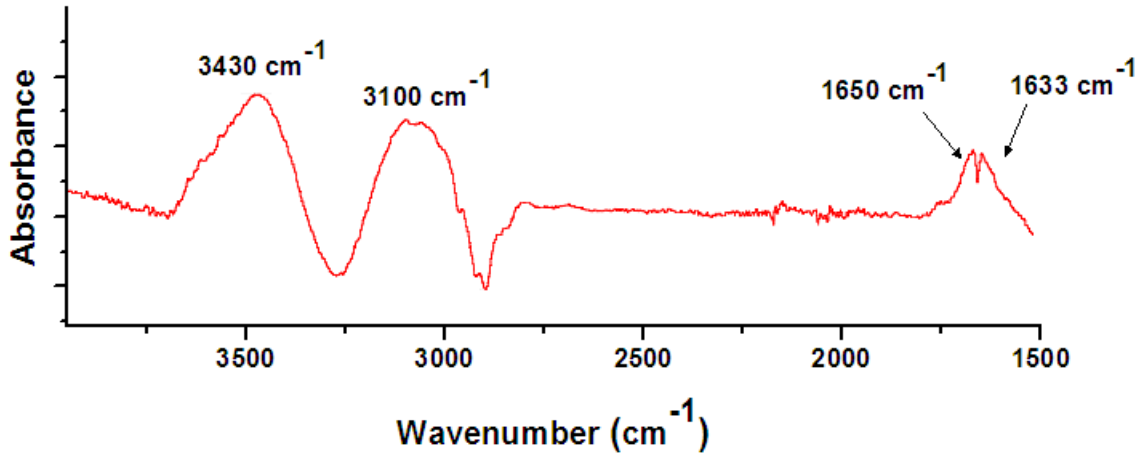

Fig 1-c. FTIR-ATR spectral subtraction between Fig 1(a) and Fig 1(b) in magnified absorbance scale.

The broad band that extends between 3600-3000 cm^{-1} (Figures 1-a and 1-b) is splitted into two adsorption peaks, as evidenced in magnified absorbance scale (Figure 1-c); the first one, detected at about 3430 cm^{-1}, is attributed to β-CD hydroxyl groups as previously discussed; actually this peak is now detectable at higher frequency. The peak wavenumbers are strictly linked to the strength of the respective H-bonds: the higher is the strength of physical or chemical interaction in which OH oscillator is involved, the more downshifted is the corresponding OH stretching frequency. The highest frequency contribution observed passing from neat β-CD (3293 cm^{-1}) to CD-lim inclusion complex (3430 cm^{-1}), suggests a reduction of hydrogen bonds between water molecules inside the β-CD cavity, as a consequence of the development of a more structured network involving the available β-CD torus-shaped cavity sites and hydrophobic D-limonene molecules [31].

The peak detected at 3100 cm^{-1} can be attributed to limonene terminal $=CH_2$ group. In addition, the peak at 1643 cm^{-1} in Figures 1-a and 1-b, is halved in two adsorption frequencies, as shown in Figure 1-c: the first one at 1650 cm^{-1} is related to water hydroxyl groups, whereas the second one at 1633 cm^{-1} concerns limonene C=C vibration mode. It is worthy to highlight that the peak of water hydroxyl groups is shifted to higher frequency if compared to neat CD; this could be due to the weakening of hydrogen bonds in the heptameric CD units upon complexation, because of both size and structural rearrangement of guest molecules within the host cavity. Probably, during the inclusion complex formation, limonene molecules lodge inside the suitable hydrophobic core of β-CD toroid, disturbing water hydrogen bonds environment and enhancing the amphiphilic character of the cyclic polysaccharide [32-33].

FTIR-ATR spectra of PBS/CD-lim 100/0 and 80/20 films are shown in Figures 2 and 3. Figures 2-a and 2-b refer to the spectral region between 4000 and 2500 cm^{-1}. Two main absorption bands are visible, namely -OH (3600-3000 cm^{-1}) and -CH- (3000-2800 cm^{-1}) bonds stretching, respectively [34]. In particular, a weak absorption near 3430 cm^{-1}, assigned to chain-end hydroxyl groups of PBS, can be observed in both samples [35]. In addition, in 80/20 composition, stronger and broaded hydroxyl group vibrational absorption can be detected, due to the presence of β-CD inside the polymeric matrix.

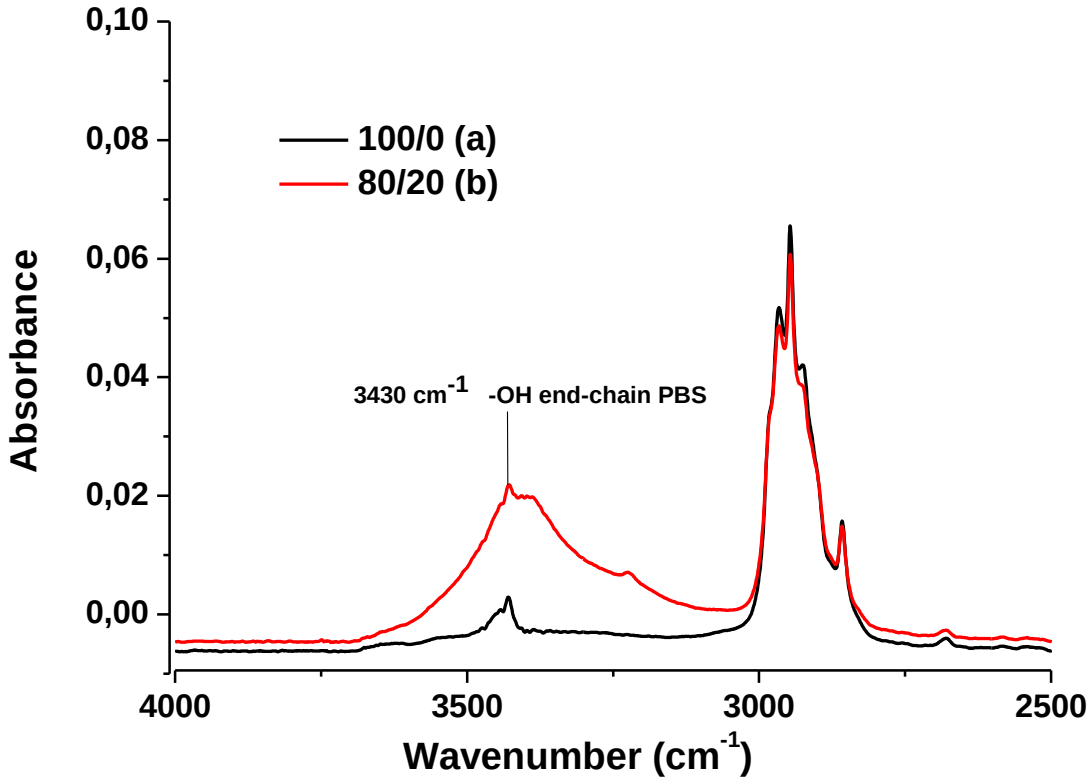

Fig 2. FTIR-ATR spectra of PBS/CD-Lim composites in the range between 4000-2500 cm^{-1}: (a) 100/0, and (b) 80/20.

In Figure 3, FTIR-ATR spectra of ester carbonyl stretching adsorption are reported. As usually evidenced in semicrystalline polyesters, the carbonyl group stretching region (-COO-) is composed of two overlapping peaks; in plain PBS spectrum there is a relatively broad band centred at approximately 1720 cm^{-1}, occurring as a shoulder of a sharper and more intense band at about 1711 cm^{-1}. Previous studies showed that the above mentioned peaks arise from the amorphous region and crystalline domain of ester carbonyl groups stretching of the polymer, respectively [36]. In Fig 3b, related to 80/20 composite, two interesting changes in carbonyl stretching modes were observed: a variation of the relative areas of the above-mentioned amorphous and crystalline regions, evaluated by a curve fitting (curves not shown), and a slight shift of PBS crystalline and amorphous bands towards higher frequencies.

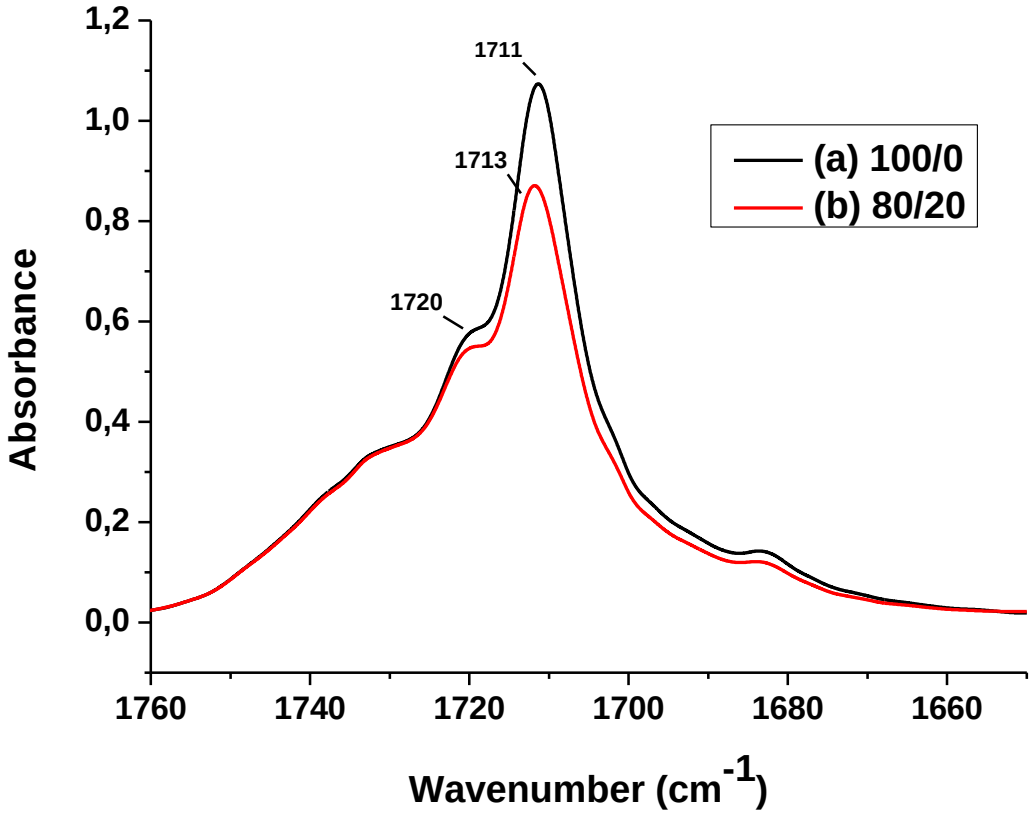

Fig 3. FTIR-ATR spectra of PBS/CD-Lim composites in the range of 1760-1660 cm^{-1}: (a) 100/0, and (b) 80/20.

The crystalline (Ca) and amorphous (Aa) peak areas of PBS carbonyl groups of different samples were quantified by using the GRAMS 8.0AI software package (Thermo Electron Corporation). The area of each peak was calculated after performing a linear background correction and assuming mixed Gaussian-Lorentzian functions.

Table 1 summarizes the exact position of carbonyl vibration peaks, the amorphous (Aa) and crystalline (Ca) region areas of all the samples and their relative ratios, with corresponding correlation factor and deviation standard.

Table 1: FTIR crystalline and amorphous peaks (cm^{-1}) and crystalline (C_a) and amorphous (A_a) areas of ester carbonyl group in 100/0, 90/10, 80/20 samples.

Ester carbonyl group (C=O)			
Sample	100/0	90/10	80/20
Crystalline peak (cm^{-1})	1711	1712	1713
Amorphous peak (cm^{-1})	1722	1722	1722
Amorphous area (A_a)	14.97	15.58	11.56
Crystalline peak area (C_a)	10.28	9.67	6.72
$A_{am}/ (A_{am} + A_{cr}) *100$	59.0	61.7	63.2
Correlation factor (R^2)	0.996	0.996	0.997
Standard Deviation	0.01	0.01	0.08

Data analysis evidences that in the composites the percentage of amorphous carbonyl band increases. In particular, the decrease in intensity of the crystalline carbonyl band in favour of a widening of the amorphous region, particularly evidenced in 80/20 composition, suggests that CD-lim inclusion complex disturbs the regular packing of PBS, resulting in a larger amorphous fraction. This outcome could be ascribed to the formation of hydrogen bond between PBS carbonyl ester group and hydroxyl residues of CD outer surfaces, which possibly complicates crystallization of PBS, as following shown by thermal analysis. This result is even more emphasized by the slight shifting of crystalline carbonyl band towards higher stretching vibration frequencies, as shown in Figure 3.

Thermogravimetry (TGA) of the CD-lim complex is illustrated in Figure 4, and compared to TGA analysis of the as-received β-cyclodextrin and D-limonene.

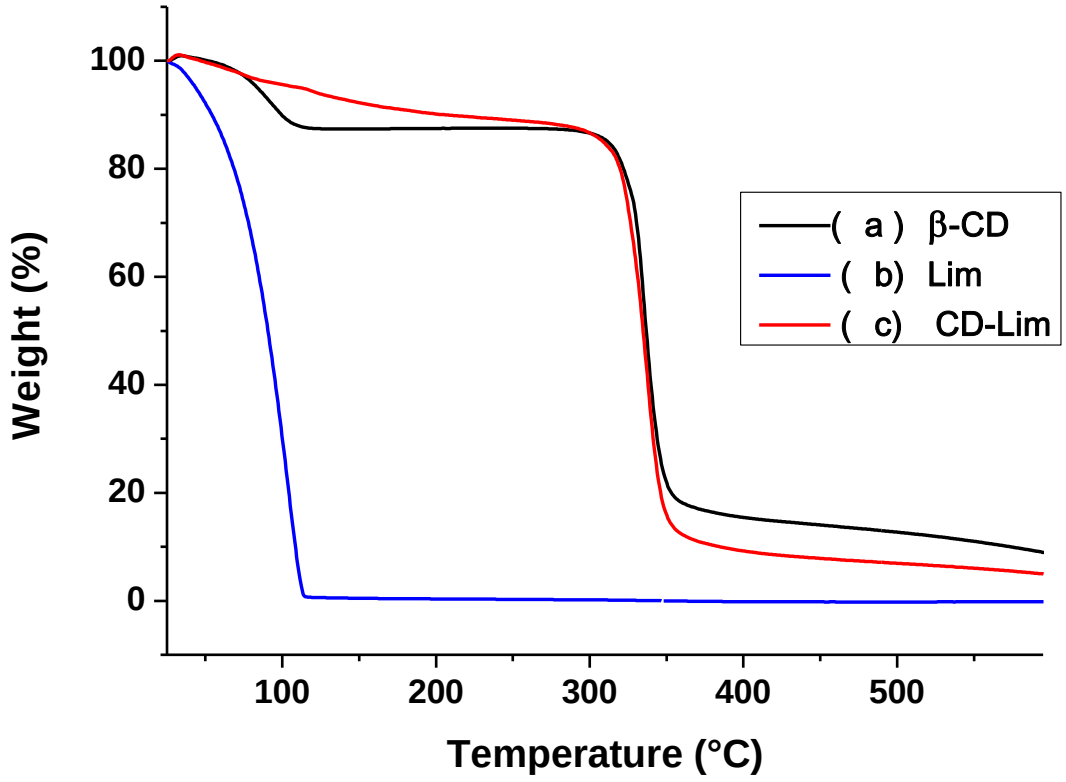

Fig 4. Thermogravimetric plots of (a) β-cyclodextrin, (b) D-limonene, (c) β-cyclodextrin limonene IC, upon heating at 20 °C/min in nitrogen atmosphere.

All the curves were normalized with respect to the initial sample weights. Upon heating at 20 °C/min, the terpene oil immediately starts to evaporate, as revealed by the continuous decrease of D-limonene amount in the sample pan, and completely volatilizes below 120 °C. The TGA curve of neat β-cyclodextrin (Fig 4a) displays multiple weight loss steps: the first one is due to release of free and freezed bound water (± 12%) up to 110°C, whereas the second one starts around 300-

350°C and is associated to a fast weight loss of about 70%. The second degradation stage is due to the depolymerizazion of cyclodextrin macromolecular chains and glucosidic rings, with formation of carbonyl group and carbon–carbon double bonds, simultaneously developing in the resulting residue (about 15%) [39]. The final thermal degradation stage (not shown in the Figure), occurs at temperatures higher than 350°C, and is linked to a slow thermal degradation of the residual char [39]. CD-lim inclusion complex (Fig 4c) displays a slower but continuous weight loss kinetics with respect to neat β-CD, from room temperature up to 300°C, where major thermal degradation of the inclusion complex starts. In the temperature range 25 – 300 °C, two degradation steps can be highlighted. The first one, ranging between 50 to 110 °C, reaches a weight loss of about 5%. Around 110 °C, a second, smoother weight loss step starts and completes around 300 °C, where the initial weight is reduced of an overall 12 % (7 % in the second stage). The end of the first degradation step coincides with both complete evaporation of D-limonene (Fig 4b) and with loss of water in plain β-cyclodextrin (Fig 4a), which at first sight complicates data interpretation.

As a matter of fact, TGA plots similar to those shown in Figure 4 for the CD-lim sample were reported for an inclusion complex of β-CD containing *p*-cymene, an essential oil whose chemical structure and steric hindrance do not differ much from limonene [40]. The two terpenes have also the same boiling point (177 °C). As detailed in Ref. [40], the first degradation step is attributed to loss of water and to possible release of a small amount of guest molecules from the samples, whereas the second gradual weight decrease is due to loss of the terpene oil encapsulated within β-CD cavity.

In other words, the data of Figure 4 evidence that, upon heating from 110 to 300 °C, about 7% of CD-lim initial weight is released, which well corresponds to the amount of D-limonene encapsulated within β-CD hollow, quantified by precipitation. This highlights that D-limonene is thermally stabilized when included within β-CD cages. More outstandingly, at 135 °C, i.e. at the processing temperature used for preparation of PBS/CD-lim samples, only a minimum fraction of D-limonene initially present in CD-lim inclusion complex is lost upon melt extrusion, and remains trapped within the cavity of the β-cyclodextrin dispersed into the PBS matrix, as revealed by the only minor weight decrease of the CD-lim sample at 135 °C specifically ascribed to loss of the terpene.

The TGA plots, upon heating of PBS and PBS/CD-lim films and their first derivatives curves (DTG) are reported in Figure 5-a and 5-b, respectively. All the curves are normalized with respect to starting sample weights.

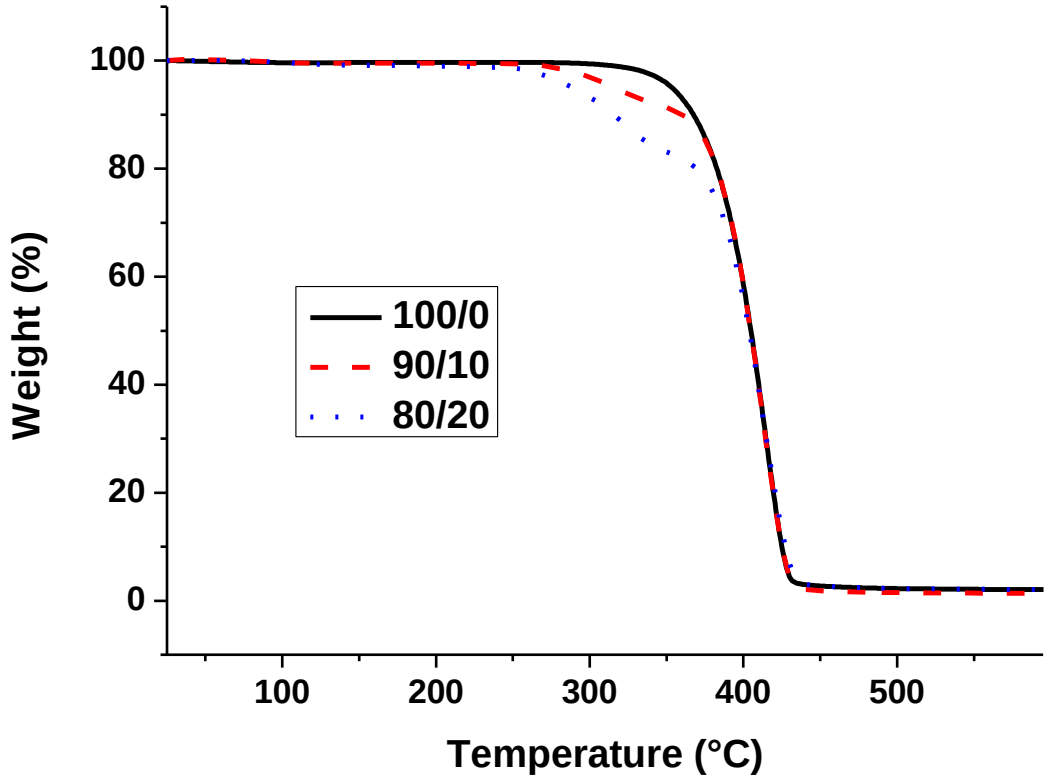

Fig 5 (a). TGA plots of PBS/CD-Lim blends: 100/0 (—), 90/10 (- - -), 80/20(…).

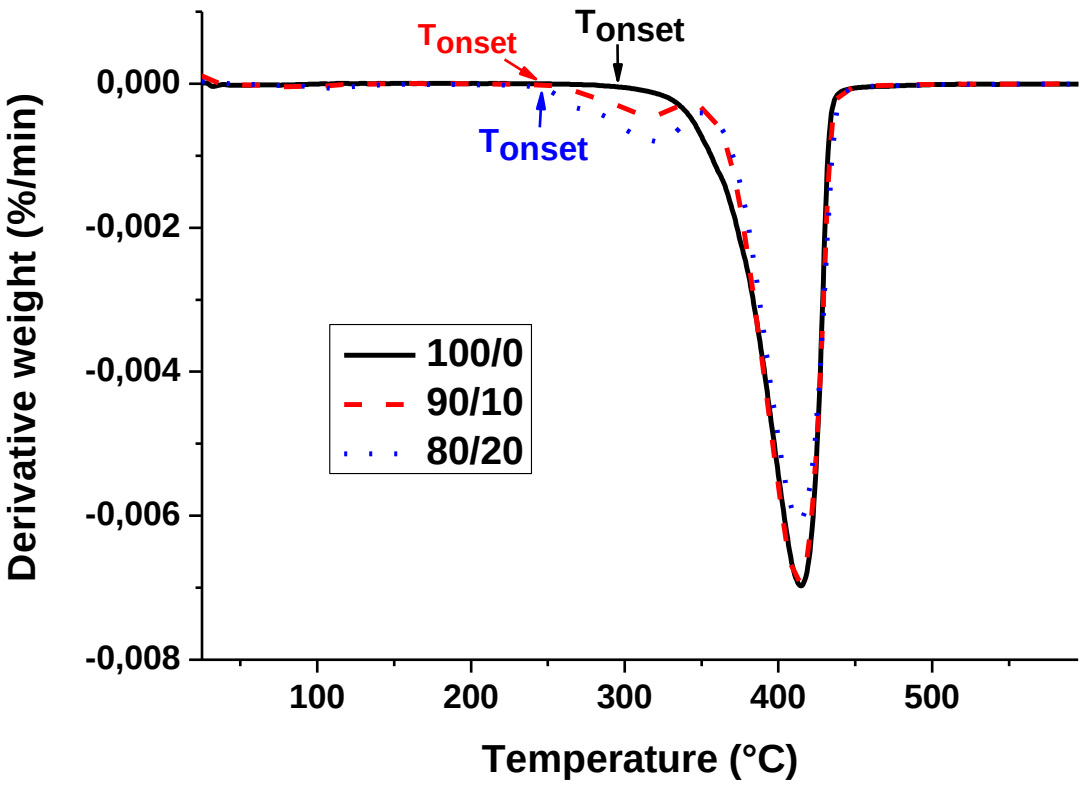

Fig 5 (b). DTG curves of PBS/CD-Lim blends: 100/0 (—), 90/10 (- - -), 80/20(…).

PBS thermogram (Fig 5a) shows no significant weight loss until 300 °C, in agreement with literature data [37]. The major degradation step is concluded at 440°C, when only 2 % of the initial sample remains. The primary weight loss is caused by volatilization of small molecules, including succinic acid that degrades at temperatures close to 200 °C, and butylene glycol that evaporates at slightly higher temperatures, below 300 °C. This decomposition is followed by major thermal degradation of PBS chains, due to random chain scission at the ester bonds, with formation of carboxylic end groups and vinyl groups [38].

As concerning PBS/CD-lim system, it is worth to observe that in presence of the inclusion complex inside polymeric matrix, the onset of degradation is anticipated of 50°C, since thermal degradation starts at about 250°C in PBS based films; moreover, analysis of DTG curves (fig 5-b) reveals two different kinetics of degradation: the first one is mostly related to inclusion complex degradation step, starting at about 250 °C and concluding at 350°C, and the second one, corresponding to main decomposition stage of the polyester, i.e. to its pyrolysis, starts at 350°C and ends at 440°C. Actually, the presence of two distinct degradation steps in PBS/CD-lim composites, may indicate that the polymeric matrix and β-CD inclusion complex are not miscible, as also

proved by DSC and optical microscopy analyses discussed below. Nevertheless, the establishment of hydrogen bonds between the polar groups of external β-CD surface and ester fraction of PBS, previously ascertained by FTIR spectroscopy, induces a mutual influence on thermal decomposition kinetics. In particular, from DTG curves, it can be emphasized that the main PBS degradation process begins at about 340°C, far beyond 40°C with respect to degradation onset temperature of neat PBS (T_{onset} at 300°C). It is then confirmed that β-CD inclusion complex disturbs the regular packing of PBS macromolecular chains; as a matter of fact, the occurrence of inter-associated hydrogen bonding can induce new polymeric steric hindrances, responsible of PBS delaying in T_{onset} of decomposition kinetic.

Further characterization of the composites structure and morphology was performed by optical microscopy and calorimetry. The optical micrographs of poly(butylene succinate), plain and blended with cyclodextrin containing limonene, are presented in Figure 6.

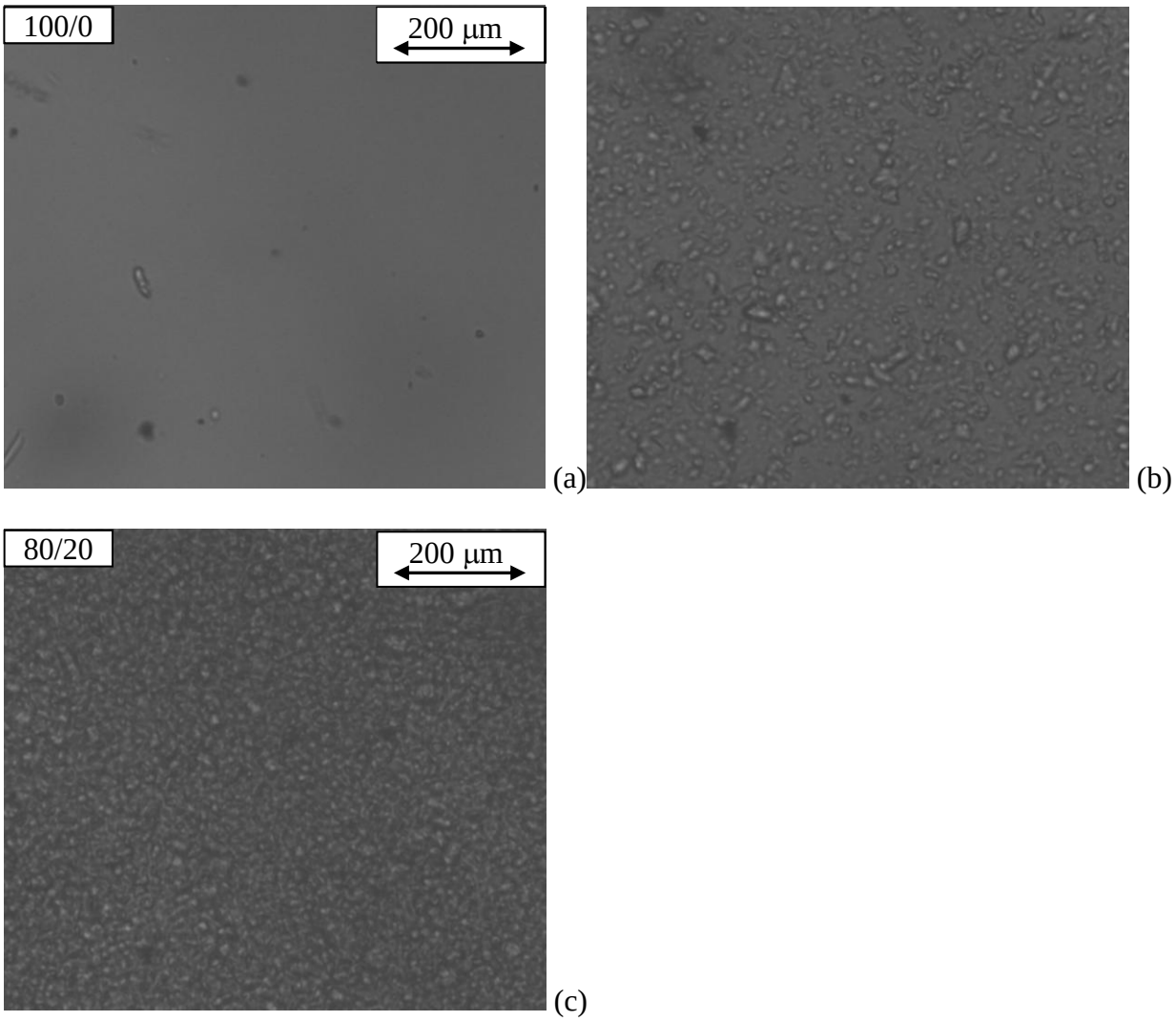

Figure 6. Optical micrographs of PBS/CD-lim composites at 135°C: (a) 100/0; (b) 90/10; (c) 80/20

Figure 6-a shows that neat PBS at 135°C is characterized by an homogeneous melt. The addition of β-cyclodextrin containing D-limonene results in a phase-separated material, with the appearance of small particles dispersed within the PBS matrix, as seen in Figures 6-b and 6-c, which show the optical micrographs of 90/10 and 80/20 systems, respectively taken at 135°C. An increase of CD-lim content results in a larger amount of dispersed droplets, as expected. The average particle size is about 1 μm. Considering that β-cyclodextrin has an outer diameter of 1.54 nm [1, 24], the optical micrographs reveal considerable aggregation of CD-lim particles upon melt mixing, likely due to the formation of particle clusters, induced by physical interaction between the polar groups of β-CD external surfaces. Moreover, the homogeneous distribution of β-CD aggregates within polymeric matrix, as evidenced in Figures 6-b and 6-c, suggests the existence of physical interaction between the components by means of hydrogen bonding.

The glass transition (T_g) of plain and doped PBS is illustrated in Figure 7.

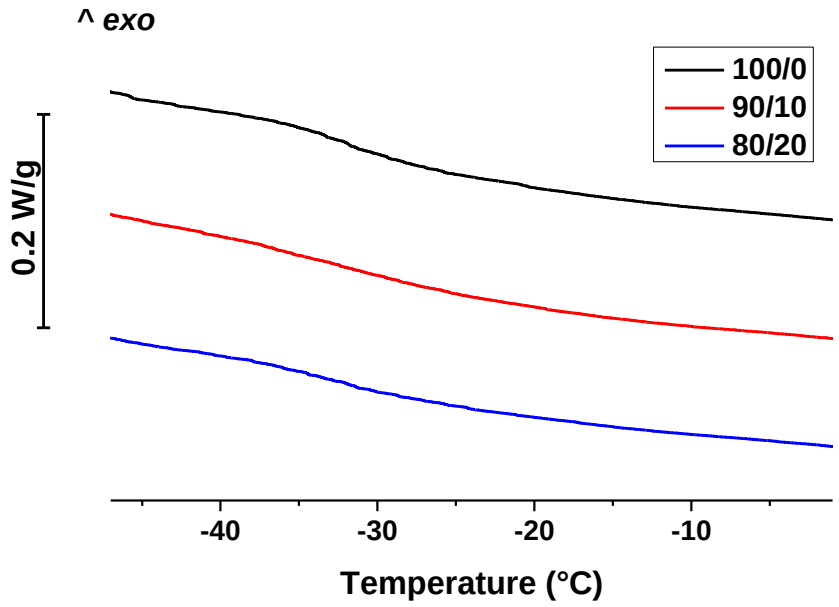

Figure 7. Glass transition temperature (T_g) of PBS based composites

Glass transition of PBS is centered at -32 °C, in agreement with literature data [41-42]. Addition of CD-lim does not shift the glass transition temperature, which remains at T_g = -32 ± 2 °C, for CD-lim content up to 20 %, but results in a slight broadening of the high temperature side of T_g range. A broadened T_g is often observed in polymer-filler systems, and is generally linked to good interfacial adhesion between the matrix and the dispersed particles, coupled with a restriction of molecular mobility of polymeric segments near the filler surface [43]. The invariance of the glass transition temperature confirms the lack of miscibility between all components, as also confirmed by the optical micrographs of Figure 6. Moreover, data of Figure 7 may support that D-limonene molecules are trapped within CD cavities, as discussed above. As a matter of fact, D-limonene is known to be an efficient plasticizer for biodegradable polyesters. For instance, it was shown that addition of 15 wt% of D-limonene to poly(lactic acid) (PLA), can lower its glass transition of about 30 °C [44-45]. The absence of T_g shifting in PBS/CD-lim based systems, proves both the lack of miscibility between PBS and CD molecules, as previously shown, and that no interaction occurs between PBS and D-limonene molecules, being the latter well trapped within β-cyclodextrin cavities.

Crystallization kinetics of PBS/CD-lim composites was analyzed both in isothermal and non-isothermal conditions. DSC thermograms gained during cooling from the melt at 4 °C/min are presented in Figure 8. Similar trends were obtained for the other cooling rates (thermograms not reported).

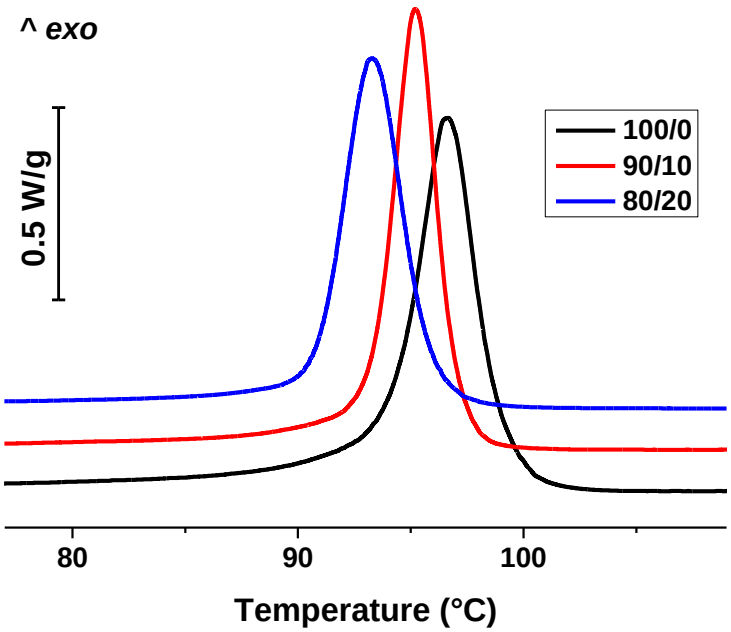

Figure 8. PBS crystallization thermograms during cooling from the melt at 4 °C/min

Crystallization of plain PBS starts around 103 °C, and is completed at circa 90 °C. Addition of the CD-lim complex delays the onset of crystallization of PBS, and results in a shift to lower temperatures of the whole crystallization exotherm.

In Figures 9-a and 9-b, the onset (T_{ons}) and peak (T_p) temperatures of the crystallization exotherms of the composites are compared in dependence of the cooling rate. The onset point was taken as the intersection of the baseline before the transition and the inflectional tangent and the peak temperature as the maximum of the exotherm [45].

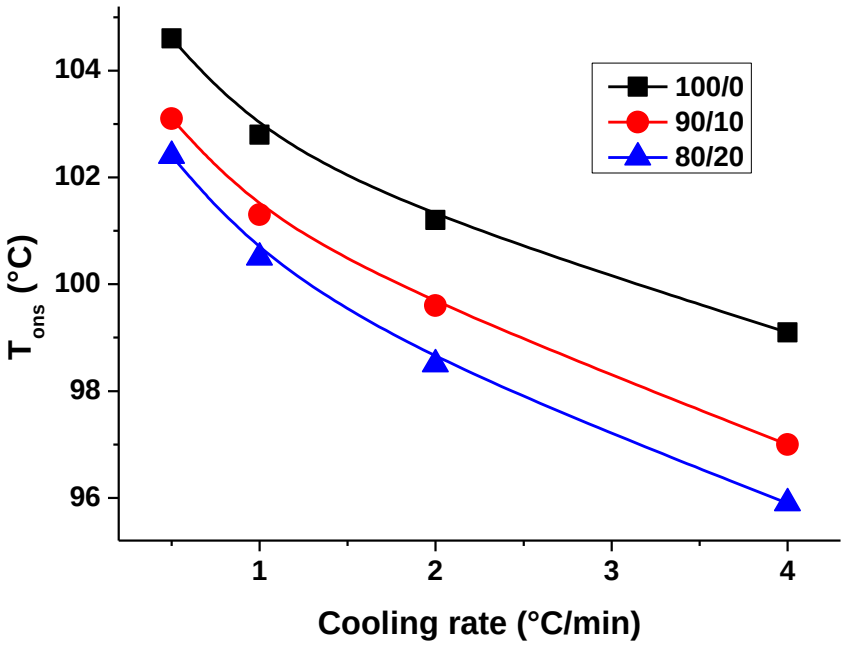

Figure 9 (a). T_{ons} of PBS crystallization exotherms as a function of cooling rate

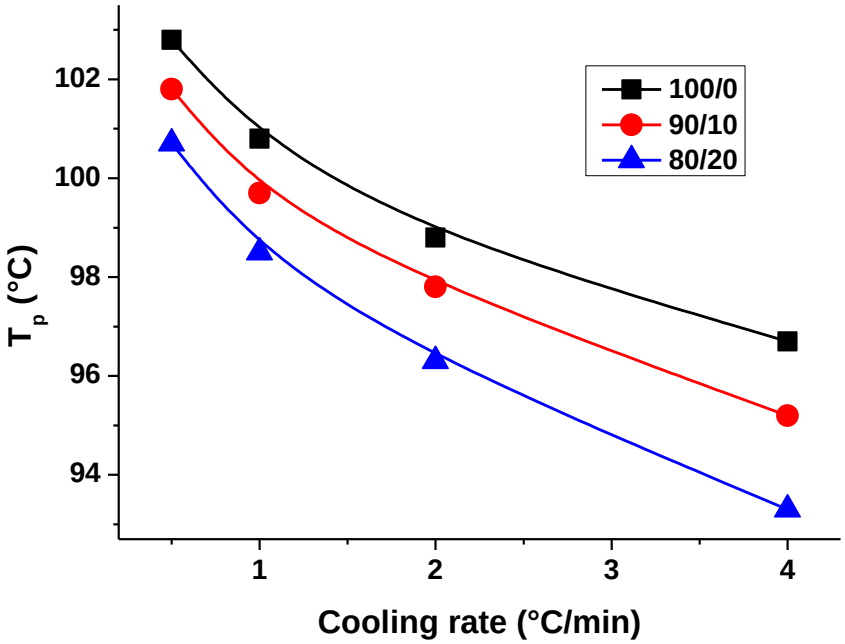

Figure 9 b T_p of PBS crystallization exotherms as a function of cooling rate

As expected, an increase in cooling rate results in a shift of the phase transition parameters of all the analyzed samples toward lower temperatures: at low cooling rates there is more time to form the nuclei, so that crystallization starts at higher temperatures [46]. Similarly, also the peak temperatures move toward lower values upon increasing the cooling rates, as result of the shift of

the whole phase transition to lower temperatures. The addition of CD-lim complex delays beginning of the phase transition, showing that, not only the solid CD-lim particles are not efficient nucleating agents able to promote the onset of PBS crystallization, but their presence disturbs chain ordering in the biodegradable polyester. Crystallization of PBS occurs in the presence of non-crystallizable CD-lim. Energy needs to be dissipated to reject, engulf or deform the dispersed particles, which causes the delayed onset and the overall shift of the phase transition to lower temperatures, at parity of cooling rate from the melt.

Crystallization kinetics of PBS/CD-lim systems was also investigated in isothermal conditions. A temperature range where all the analyzed compositions crystallize in a reasonable time was selected, to better compare the crystallization behavior of the various samples. The heat evolved during crystallization of PBS was recorded as a function of time, and the fraction of material crystallized after a period of time t (X_t) was calculated from the ratio of the heat generated at time t and the total heat developed during the phase transformation. Plotting X_t against time, the half-time of crystallization ($\tau_{1/2}$), defined as the time needed for 50 % the final crystallinity to develop, was obtained. The $\tau_{1/2}$ values of the analyzed PBS/CD-lim composites are reported in Figure 10 as a function of the crystallization temperature (T_c).

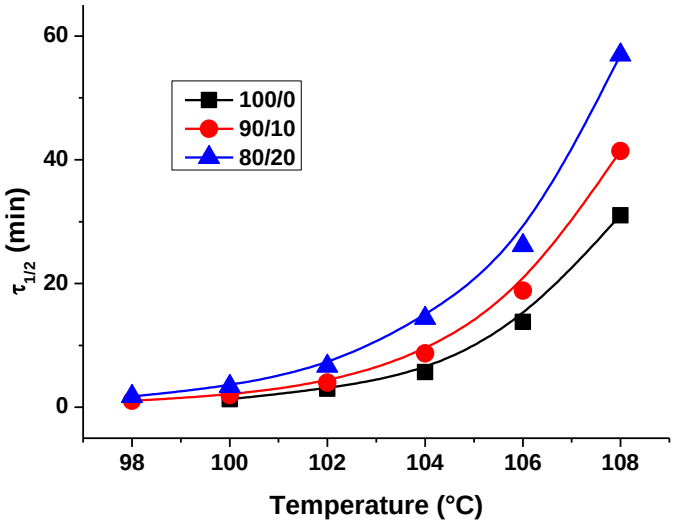

Figure 10. Half-time crystallization ($\tau_{1/2}$) of PBS exotherms as a function of temperature

As expected, in the analyzed range, the phase transition rate decreases with T_c. More importantly, Figure 10 reveals that longer crystallization times are attained by PBS in the composites, compared to the plain polymer, confirming the results of non-isothermal crystallization analyses, which revealed that the addition of CD-lim delays crystallization of PBS.

The influence of CD-lim on melting behavior of PBS is illustrated in Figure 11, which reports the DSC traces of the three analyzed compositions upon heating at 20 °C/min after isothermal crystallization at 100 °C.

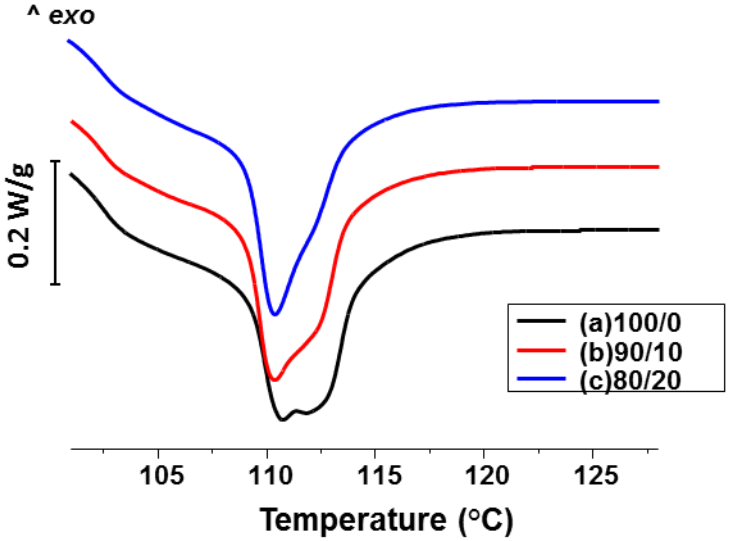

Figure 11 Melting thermograms of PBS upon heating at 20 °C/min after isothermal crystallization at 100 °C.

Plain PBS displays a multiple melting behavior, with three main endothermic events: a weak one, centered around 103°C and a major endotherm with two close peaks at 111 and 112.5 °C. The multiple melting behavior of PBS has been investigated by a number of authors, and is generally ascribed to the existence of multiple lamellae populations developed upon isothermal crystallization, coupled with partial melting and recrystallization processes [42, 47-50]. Addition of CD-lim affects only slightly the multiple melting of PBS: the small endotherm located a few degrees above the isothermal crystallization temperature, typical not only of PBS, but also of a number of other semicrystalline polymers [51-55] remains mostly unaffected by the presence of the filler. Conversely, the two minima of the major endotherm slightly vary in size and position. Indeed, the peak at 111 °C in plain PBS moves to a somewhat lower temperature and becomes predominant in the systems containing CD-lim, whereas the high temperature peak appears as a shoulder in the major melting event, but occurs at the same temperature as in the plain PBS. Data shown in Figure 10 support the discussion of the multiple melting of PBS appeared in the literature: the small endotherm just above T_c, whose origin is highly debated, being ascribed either to melting of secondary or more defective lamellae, or to enthalpy relaxation of the rigid amorphous fraction,

appears unaffected by the presence of CD-lim [51-55]. The peak at 111 °C, which is usually ascribed to fusion of primary lamellae [47-49] moves to lower temperature when CD-lim is present, this experimental evidence may result from the hindering effect of the filler on crystallization of PBS, which may lead to thinner or more defective lamellae that melt at somewhat lower temperatures upon heating. The final endotherm refers to melting of the crystal lamellae that have perfected and/or recrystallized into more stable structures. Their melting temperature is not determined by the thermal stability of the original crystals, but only by the DSC scanning rate, which determines the extent of crystal reorganization during heating. PBS crystals, heated at the same rate after isothermal crystallization, melt at the same temperature in plain PBS and in the analyzed PBS/CD-lim based films, which supports the view of a partial melting and recrystallization process, possibly coupled with crystal perfection upon heating [45].

Conclusions

In this paper, structural morphological and thermal properties of poly(butylene succinate) (PBS) and inclusion complex of β-cyclodextrins and D-limonene based composites were investigated, in order to obtain films potentially exploitable as novel bio-active food packaging materials.

FTIR and TGA analysis evidenced that D-limonene was efficiently encapsulated inside β-CD cavities, since the inclusion complex obtained was thermally stable up to the onset of β-CD degradation temperature. Moreover, β-CD-Lim complex affected thermal stability of PBS, because of the hydrogen bonding occurring between polar groups of β-CD-lim and functional groups of PBS, as evidenced by FTIR and DTG analysis. Furthermore, optical micrographs of PBS based systems highlighted a phase-separated material even if, the existence of physical interaction between polar groups induced a homogeneous and fine distribution of particles within polymeric matrix. From the analysis of DSC data it was highlighted both the immiscibility of the components, and the anti.-nucleating action exerted by β-CD-lim complex towards PBS, evidenced by a strong delaying in kinetics of PBS crystallization process

Acknowledgements

The authors gratefully thank Dr. Giacomo Cesaro, industrial designer, for its skilful support in performing the graphical abstract; the authors acknowledge also the project SOFIA, in the frame of

National Technological Cluster of Ministry of University and Research (MIUR), for the financial support.

References

1. J. Szejtli, Introduction and General Overview of Cyclodextrin Chemistry, Chem. Rev. 98, (1998) 1743-1753, http://pubs.acs.org/doi/pdf/10.1021/cr970022c.
2. T. Dong, W Kai, P. Pan, A. Cao, Y. Inoue, Effects of Host-Guest Stoichiometry of R-Cyclodextrin-Aliphatic Polyester Inclusion Complexes and Molecular Weight of Guest Polymer on the Crystallization Behavior of Aliphatic Polyesters, Macromolecules, 40, (2007) 7244-7251, http://pubs.acs.org/doi/abs/10.1021/ma071374g.
3. M. Wei, X. Shuai, A E. Tonelli, Melting and Crystallization Behaviors of Biodegradable Polymers Enzymatically Coalesced from Their Cyclodextrin Inclusion Complexes, Biomacromolecules, 4, (2003) 783-792, http://pubs.acs.org/doi/abs/10.1021/bm034078u.
4. Shuai, X.; Porbeni, F. E.; Wei, M.; Shin, I. D.; Tonelli, A. E. Macromolecules, 34, (2001) 7355, http://pubs.acs.org/doi/pdf/10.1021/ma0109626.
5. Shuai, X.; Wei, M.; Porbeni, F. E.; Bullions, T. A.; Tonelli, A. E. Biomacromolecules, 3, (2002) 201-207, http://pubs.acs.org/doi/pdf/10.1021/bm015609m.
6. Huang, L.; Gerber, M.; Taylor, H.; Lu, J.; Tapaszi, E.; Wutkowski, M.; Hill, M.; Lewis, C.; Harvey, A.; Herndon, A.; Wei, M.; Rusa, C. C.; Tonelli, A. E. Macromol. Chem. Symp., 176, (2001) 129-144, http://onlinelibrary.wiley.com/doi/10.1002/1521-3900(200112)176:1%3C129
7. J.F. Mano, Thermal Behaviour and Glass Transition Dynamics of Inclusion Complexes of α-Cyclodextrin with Poly(D,L-lactic acid), Macromol. Rapid Commun., 29, (2008) 1341–1345, http://onlinelibrary.wiley.com/doi/10.1002/marc.200800180.
8. R Zhang, Y. Wang, K. Wang, G. Zheng, Q. Li, C. Shen, Crystallization of poly(lactic acid) accelerated by cyclodextrin complex as nucleating agent, Polym. Bull., 70, (2013), 195–206, DOI 10.1007/s00289-012-0814-y
9. Y.He, Y.Inoue, α-Cyclodextrin-Enhanced Crystallization of Poly(3-hydroxybutyrate), Biomacromolecules, 4, (2003), 1865-1867, http://pubs.acs.org/doi/full/10.1021/bm034260v.
10. X Shuai, F E. Porbeni, M Wei, T Bullions, A E. Tonelli, Stereoselectivity in the Formation of Crystalline Inclusion Complexes of Poly(3-hydroxybutyrate)s with Cyclodextrins, Macromolecules, 35, (2002), 3778-3780, http://pubs.acs.org/doi/pdf/10.1021/ma012038h.
11. T .Dong, Y. He, B. Zhu, K-M Shin, Y Inoue, Nucleation Mechanism of R-Cyclodextrin-Enhanced Crystallization of Some Semicrystalline Aliphatic Polymers, Macromolecules, 38, (2005), 7736-7744, http://pubs.acs.org/doi/pdf/10.1021/ma050826r.
12. C. C. Rusa , C. Luca, and A. E. Tonelli, Polymer-Cyclodextrin Inclusion Compounds: Toward New Aspects of Their Inclusion Mechanism, Macromolecules, 34, (2001), 1318–1322, http://pubs.acs.org/doi/pdf/10.1021/ma001868c.

13. K. K. Aggarwal, S. P. S. Khanuja, A Ahmad, T. R. Santha Kumar, V K. Gupta, S Kumar, Antimicrobial activity profiles of the two enantiomers of limonene and carvone isolated from the oils of *Mentha spicata* and *Anethum sowa*, Flavour Fragr. J. 17, (2002) 59–63, http://onlinelibrary.wiley.com/doi/10.1002/ffj.1040/epdf.
14. Rančić, A., Soković, M., Van Griensven, L., Vukojević, J., Brkić, D., & Ristić, M. Antimicrobial activity of limonene. Matieres Medicales, 23, (2003), 83-88, http://www.mocbilja.rs/lekovitesirovine/pdf/10_Originalni_ls_23_07.pdf
15. Z Zhang, F Vriesekoop, Q Yuan, H Liang, Effects of nisin on the antimicrobial activity of D-limonene and its nanoemulsion, Food Chemistry 150, (2014), 307–312 http://dx.doi.org/10.1016/j.foodchem.2013.10.160.
16. Fleming-Jones, M. E., & Smith, R. E., Volatile organic compounds in foods: A five year study. Journal of Agriculture and Food Chemistry, 51, 27, (2003), 8120–8127, http://pubs.acs.org/doi/pdf/10.1021/jf0303159.
17. Gutierrez, J., Barry-Ryan, C., & Bourke, P., Antimicrobial activity of plant essential oils using food model media: Efficacy, synergistic potential and interactions with food components, Food Microbiology, 26, 2, (2009), 142–150, doi:10.1016/j.fm.2008.10.008.
18. Lv, F., Liang, H., Yuan, Q., & Li, C, In vitro antimicrobial effects and mechanism of action of selected plant essential oil combinations against four food-related microorganisms, Food Research International, 44, 9, (2011), 3057–3064, doi:10.1016/j.foodres.2011.07.030.
19. J. Sun, D-limonene: Safety and clinical applications, Alternative Medicine Review, 12, (2007), 259-264, http://www.anaturalhealingcenter.com/documents/Thorne/articles/Limonene12-3.pdf
20. Chikhoune, A., Hazzit, M., Kerbouche, L., Baaliouamer, A., & Aissat, K., Tetraclinis articulata (Vahl) Masters essential oils: Chemical composition and biological activities, J. Essent. Oil Res., 25, (2013), 300-307, http://www.tandfonline.com/doi/abs/10.1080/10412905.2013.774625.
21. Settanni, L., Palazzolo, E., Guarrasi, V., Aleo, A., Mammina, C., Moschetti, G., et al., Inhibition of foodborne pathogen bacteria by essential oils extracted from citrus fruits cultivated in Sicily. Food Control, 26, 2, (2012), 326–330, doi:10.1016/j.foodcont.2012.01.050.
22. Li, P. H., & Chiang, B. H. Process optimization and stability of D-limonene-in-water nanoemulsions prepared by ultrasonic emulsification using response surface methodology, Ultrasonics Sonochemistry, 19, 1, (2012), 192–197, doi:10.1016/j.ultsonch.2011.05.017.
23. J Xu, B-H Guo, Poly(butylene succinate) and its copolymers: Research, development and industrialization, Biotechnol. J. 5, 2010, 1149–1163. http://onlinelibrary.wiley.com/doi/10.1002/biot.201000136/epdf.

24. Reineccius, G.A., Flavor encapsulation, Food Review Intern, 5, (1989), 147-176 http://www.tandfonline.com/doi/abs/10.1080/87559128909540848.
25. B R. Bhandari, B R. D'Arcy, L L Thi Bich, Lemon Oil to β-Cyclodextrin Ratio Effect on the Inclusion Efficiency of β-Cyclodextrin and the Retention of Oil Volatiles in the Complex, J. Agric. Food Chem., 46, (1998) 1494-1499 http://pubs.acs.org/doi/pdf/10.1021/jf970605n.
26. Vyazovkin, S., Chrissafis, K., Di Lorenzo, M.L., Koga, N., Pijolat, M., Roduit, B., Sbirrazzuoli, N., Suñol, J.J., ICTAC Kinetics Committee recommendations for collecting experimental thermal analysis data for kinetic computations, Thermochimica Acta, 590, (2014) 1-23 http://dx.doi.org/10.1016/j.tca.2014.05.036.
27. Di Lorenzo ML, Cimmino S, Silvestre C, Nonisothermal Crystallization of Isotactic Polypropylene Blended with Poly(α-pinene). I. Bulk Crystallization, J Appl Polym Sci 82, (2001), 358-367 http://onlinelibrary.wiley.com/doi/10.1002/app.1859/epdf.
28. O. Egyed and V. Weiszfeiler Structure determination of copper (II) -β-cyclodextrin complex by Fourier transform infrared spectroscopy. Vibrational Spectroscopy, 7, (1994), 73-77, http://ac.els-cdn.com/0924203194850429/1-s.
29. Wei Li, Bitai Lu, Aiguo Sheng, Feng Yang, Zhendong Wang, Spectroscopic and theoretical study on inclusion complexation of beta-cyclodextrin with permethrin, Journal of Molecular Structure, 981, (2010), 194–203, doi:10.1016/j.molstruc.2010.08.008.
30. M. Wei, A. E. Tonelli, Compatiblization of Polymers via Coalescence from Their Common Cyclodextrin Inclusion Compounds, Macromolecules, 34, (2001), 4061 http://pubs.acs.org/doi/pdf/10.1021/ma010235a.
31. Thomas Steiner and Gertraud Koellner, Crystalline P-Cyclodextrin Hydrate at Various Humidities: Fast, Continuous, and Reversible Dehydration Studied by X-ray Diffraction, Journal of American Chemical Society, 116, (1994), 5122-5128 http://pubs.acs.org/doi/pdf/10.1021/ja00091a014
32. I. Bratu, A. Hernanz, J. M. Gavira, G H. Bora, FT-IR Spectroscopy of inclusion complexes of β-cyclodextrin with fenbufen and ibuprofen, Romanian Journal of Physics, 50, 9 –10, (2005), 1063–1069, http://www.nipne.ro/rjp/2005_50_9-10/1063_1070.pdf.
33. V. Crupi, R. Ficarra, M. Guardo, D. Majolino, R. Stancanelli, V. Venuti , UV–vis and FTIR–ATR spectroscopic techniques to study the inclusion complexes of genistein with β –cyclodextrins, Journal of Pharmaceutical and Biomedical Analysis, 44, 2007, 110–117 doi:10.1016/j.jpba.2007.01.054.
34. Stuart BH. Infrared spectroscopy: fundamentals and applications. Hoboken: Wiley; 2004, http://www.kinetics.nsc.ru/chichinin/books/spectroscopy/Stuart04.pdf

35. Structure and Properties of Alkaline Lignin-filled Poly(butylene succinate) Plastics, Dongkuan Fan, Peter R Chang, Ning Lin, Jiahui Yu and Jin Huang, Iranian Polymer Journal, 20, 1, (2011), 3-14, http://www.sid.ir/en/VEWSSID/J_pdf/813201112701.pdf.
36. Tungalag Dong, Yong He, Kyung-moo Shin, Yoshio Inoue, Formation and Characterization of Inclusion Complexes of Poly(butylene succinate) with α- and γ-Cyclodextrins, Macromolecular Bioscience, 4, (2004), 1084-1091, http://onlinelibrary.wiley.com/doi/10.1002/mabi.200400054/epdf.
37. K. Chrissafis, K.M. Paraskevopoulos, D.N. Bikiaris, Thermal degradation mechanism of poly(ethylene succinate) and poly(butylene succinate): Comparative study, Thermochimica Acta, 435, (2005), 142–150, doi:10.1016/j.tca.2005.05.011.
38. L.H. Buxbaum, Angew, Chem. Int. Ed. 7, (1968), 182- doi: 10.1002/anie.196801821.
39. Francesco Trotta, Marco Zanetti, Giovanni Camino *Thermal degradation of cyclodextrins* Polymer Degradation and Stability 69, (2000), 373-379, PII: S0141-3910(00)00084-7.
40. M. R. Serafini, P. P. Menezes, L. P. Costa, C. M. Lima, L. J. Quintans Jr, J. C. Cardoso, J. R. Matos, J. L. Soares-Sobrinho, S. Grangeiro Jr, P. S. Nunes, L. R. Bonjadim, A. A. S. Araújo, Interaction of *p*-cymene with β-cyclodextrin, J Therm Anal Calorim, 109, (2012), 951–955 doi10.1007/s10973-011-1736-x.
41. Z Gan, H Abe, H Kurokawa, Y Doi, Solid-State Microstructures, Thermal Properties, and Crystallization of Biodegradable Poly(butylene succinate) (PBS) and Its Copolyesters, Biomacromolecules, 2, 2001, 605-613, http://pubs.acs.org/doi/pdf/10.1021/bm015535e.
42. F. Signori, M. Pelagaggi, S. Bronco, M. C. Righetti, Amorphous/crystal and polymer/filler interphases in biocomposites from poly(butylene succinate), Thermochimica Acta, 543, (2012), 74–81, http://dx.doi.org/10.1016/j.tca.2012.05.006.
43. P B. Messersmith, E. P. Giannelis, Synthesis and Characterization of Layered Silicate-Epoxy Nanocomposites, Chem. Mater., 6, (1994), 1719-1725, doi: 10.1021/cm00046a026.
44. M P. Arrieta, J. López, A. Hernández, E. Rayón, Ternary PLA–PHB–Limonene blends intended for biodegradable food packaging applications, Europ. Polym. J, 50, (2014), 255–270, http://dx.doi.org/10.1016/j.eurpolymj.2013.11.009.
45. Wunderlich, B. Thermal Analysis; Academic Press: New York, 1990 ISBN 0-12-765605-7
46. Di Lorenzo, M. L.; Silvestre, C., Prog Polym Sci, Non isothermal crystallization of polymers, 24, (1999), 917-950, PII: S0079-6700(99)00019-2.
47. E. S. Yoo, S. S. Im, Melting Behavior of Poly(butylene succinate) during Heating Scan by DSC, Journal of Polymer Science: Part B: Polymer Physics, 37, (1999), 1357–1366, doi: 10.1002/(SICI)1099-0488(19990701)37.

48. Z Qiua, M Komura, T Ikehara, T Nishi, DSC and TMDSC study of melting behaviour of poly(butylene succinate) and poly(ethylene succinate), Polymer, 44 (2003) 7781–7785, doi:10.1016/j.polymer.2003.10.045.
49. X Wang , J Zhou, L Li, Multiple melting behavior of poly(butylene succinate), European Polymer Journal, 43, (2007), 3163–3170, doi:10.1016/j.eurpolymj.2007.05.013.
50. M E. Makhatha, S Sinha Ray, J Hato, A S. Luyt, M Bousmina, Thermal and Thermomechanical Properties of Poly(butylene succinate) Nanocomposites, J Nanosci Nanotech, 8, (2007), 1–11, doi: 10.1166/jnn.2008.017.
51. Xu X, Ince S, Cebe P., Development of the crystallinity and rigid amorphous fraction in cold-crystallized isotactic polystyrene, J. Polym Sci Part B: Polym Phys., 41, (2003), 3026–36, doi: 10.1002/polb.10625.
52. Xu H, Cebe P., Heat capacity study of isotactic polystyrene: dual reversing crystal melting and relaxation of rigid amorphous fraction, Macromolecules, 37, (2004), 2797–2806 http://pubs.acs.org/doi/pdf/10.1021/ma035961n.
53. Righetti MC, Di Lorenzo ML, Tombari E, Angiuli M., The low temperature endotherm in poly(ethylene terephthalate): partial melting and rigid amorphous fraction mobilization, J. Phys. Chem. B. 112, (2008), 4233–4241, http://pubs.acs.org/doi/pdf/10.1021/jp076399w.
54. Di Lorenzo ML. The melting process and the rigid amorphous fraction of cis-1,4-polybutadiene, Polymer, 50, (2009), 578–584, doi:10.1016/j.polymer.2008.11.025.
55. Righetti MC, Tombari E, Di Lorenzo ML., The role of the crystallization temperature on the nanophase structure evolution of poly[(R)-3-hydroxybutyrate], J. Phys. Chem. B.;117, 40, (2013), 12303–12311, doi.org/10.1021/jp4063127. |

Table

Table 1
FTIR crystalline and amorphous peaks (cm^{-1}) and crystalline (C_a) and amorphous (A_a) areas of ester carbonyl group in 100/0, 90/10, 80/20 samples

Ester carbonyl group (C=O)			
Sample	100/0	90/10	80/20
Crystalline peak (cm^{-1})	1711	1712	1713
Amorphous peak (cm^{-1})	1722	1722	1722
Amorphous area (A_a)	14.97	15.58	11.56
Crystalline peak area (C_a)	10.28	9.67	6.72
$A_{am}/ (A_{am} + A_{cr}) *100$	59.0	61.7	63.2
Correlation factor (R^2)	0.999	0.996	0.997
Standard Deviation	0.01	0.01	0.08

Figure(s)

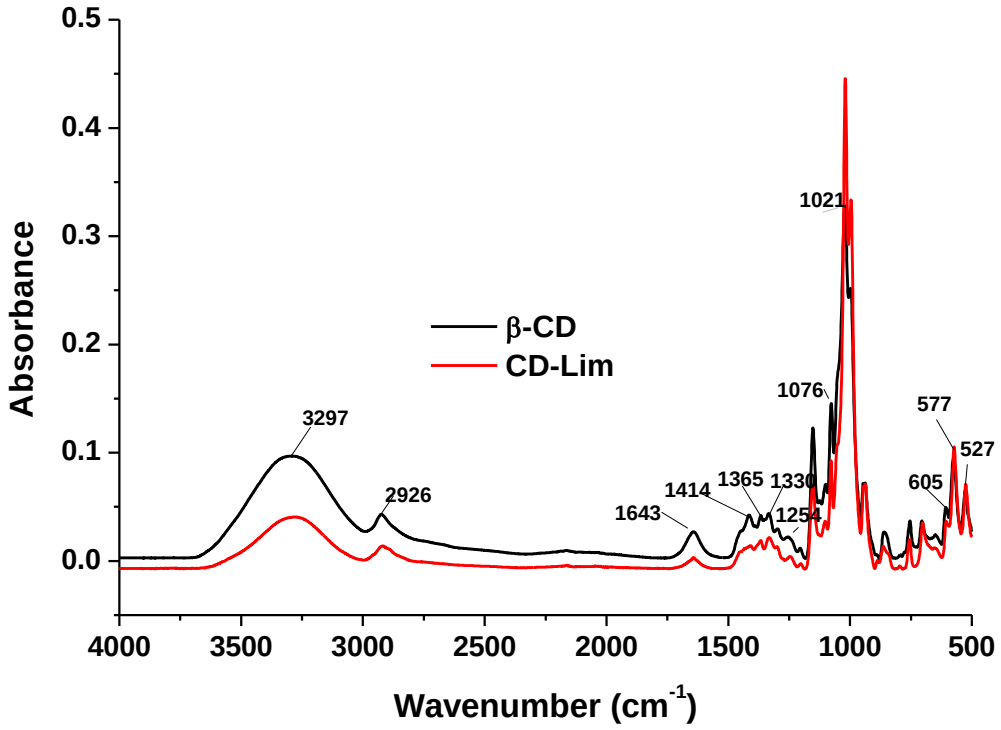

Fig 1. FTIR-ATR spectra of: (a) β-CD, and (b) CD-Lim inclusion complex.

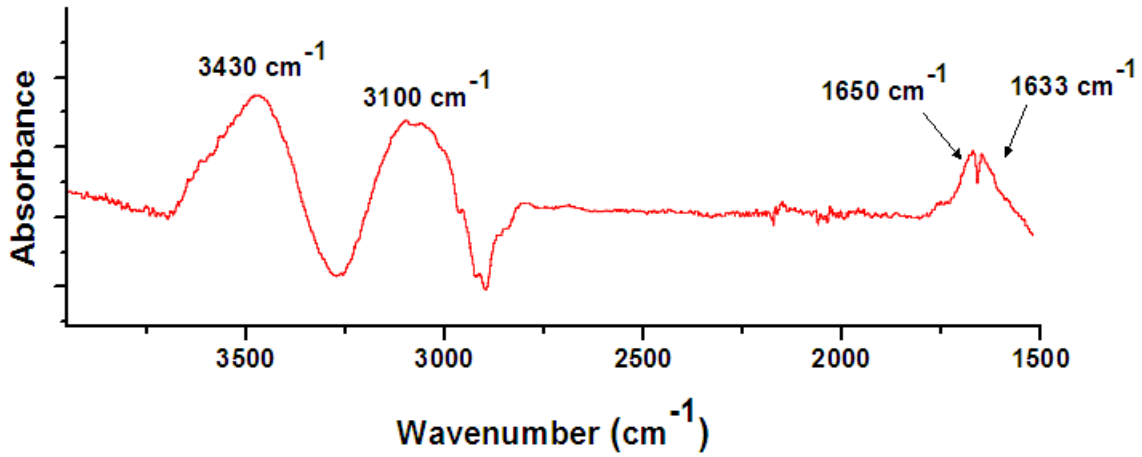

Fig 1-c. FTIR-ATR spectral subtraction between Fig 1(a) and Fig 1(b) in magnified absorbance scale.

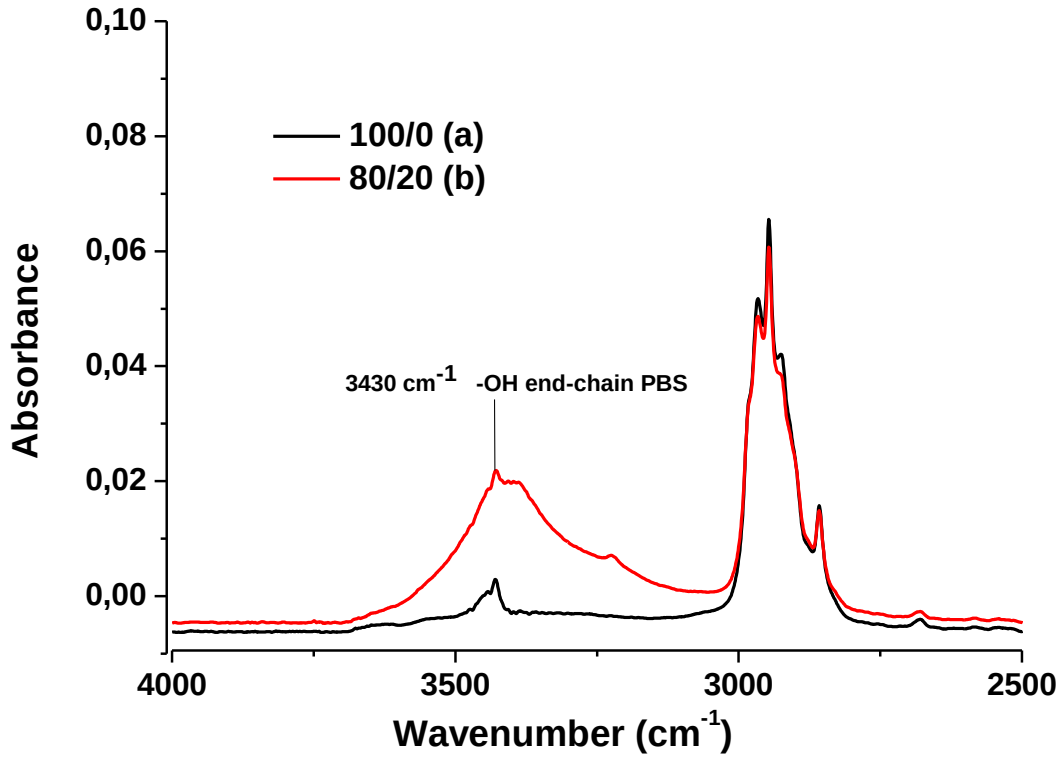

Fig 2. FTIR-ATR spectra of PBS/CD-Lim composites in the range between 4000-2500 cm^{-1}: (a) 100/0, and (b) 80/20.

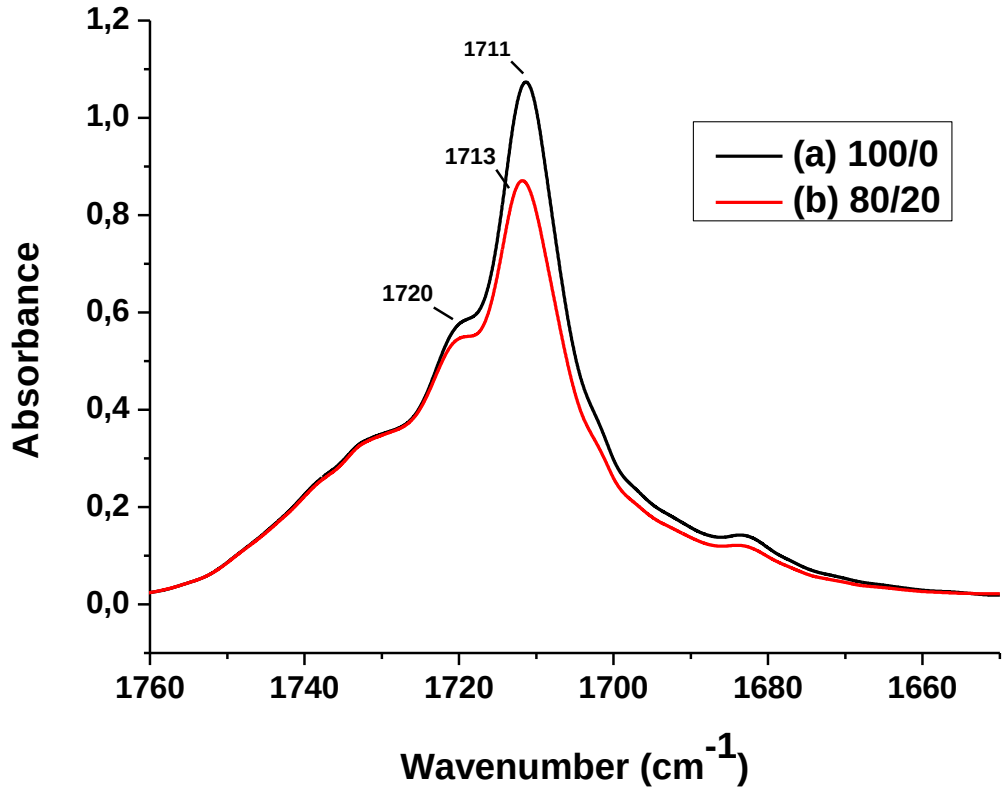

Fig 3. FTIR-ATR spectra of PBS/CD-Lim composites in the range between 1760-1660 cm^{-1}: (a) 100/0, and (b) 80/20.

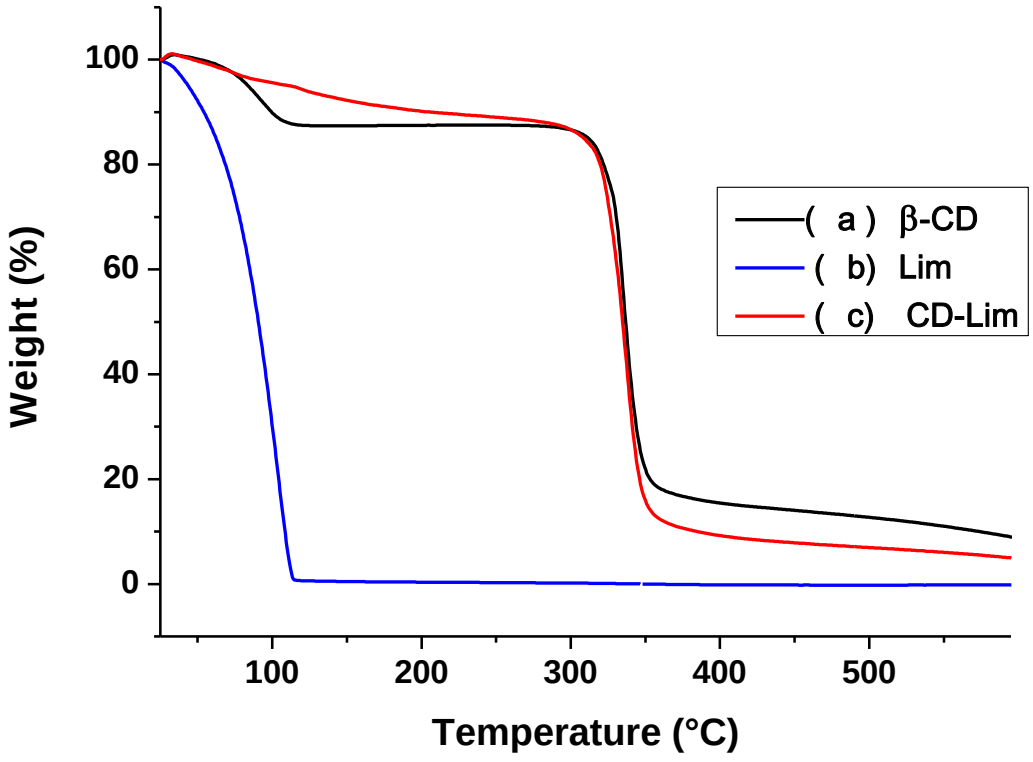

Fig 4. Thermogravimetric curves of (a) β-cyclodextrin, (b) D-limonene, (c) β-cyclodextrin limonene IC, upon heating at 20 °C/min in nitrogen atmosphere.

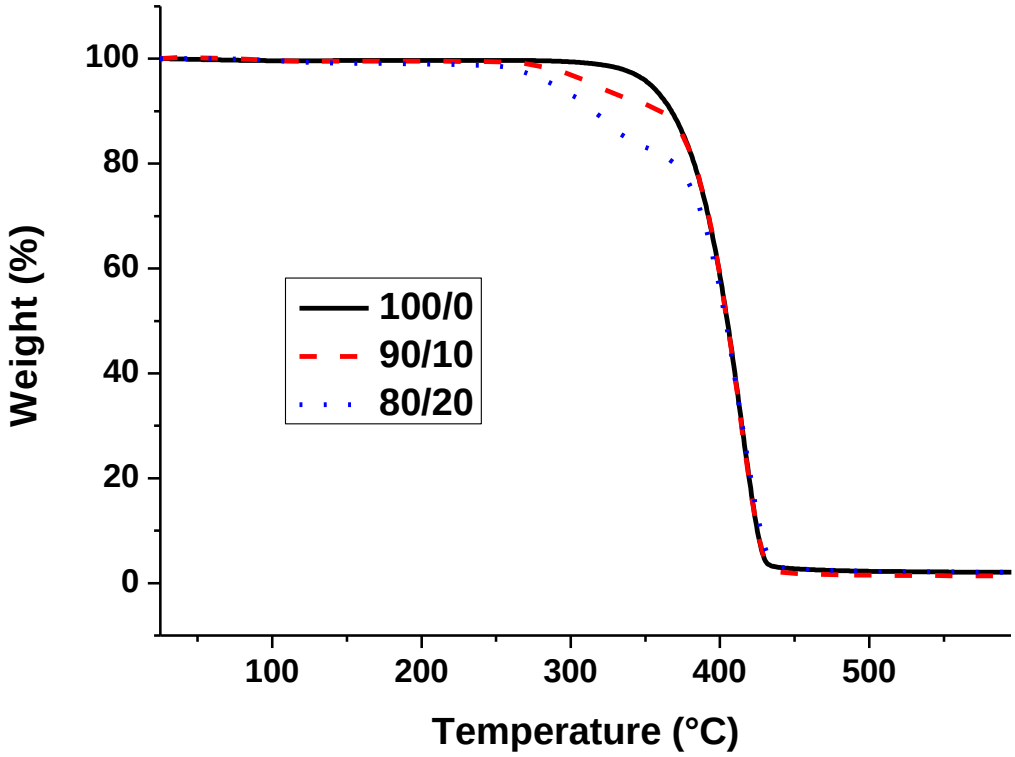

Fig 5 (a) Thermogravimetric curves of PBS/CD-Lim blends: 100/0 (—), 90/10 (- - -), 80/20(…)

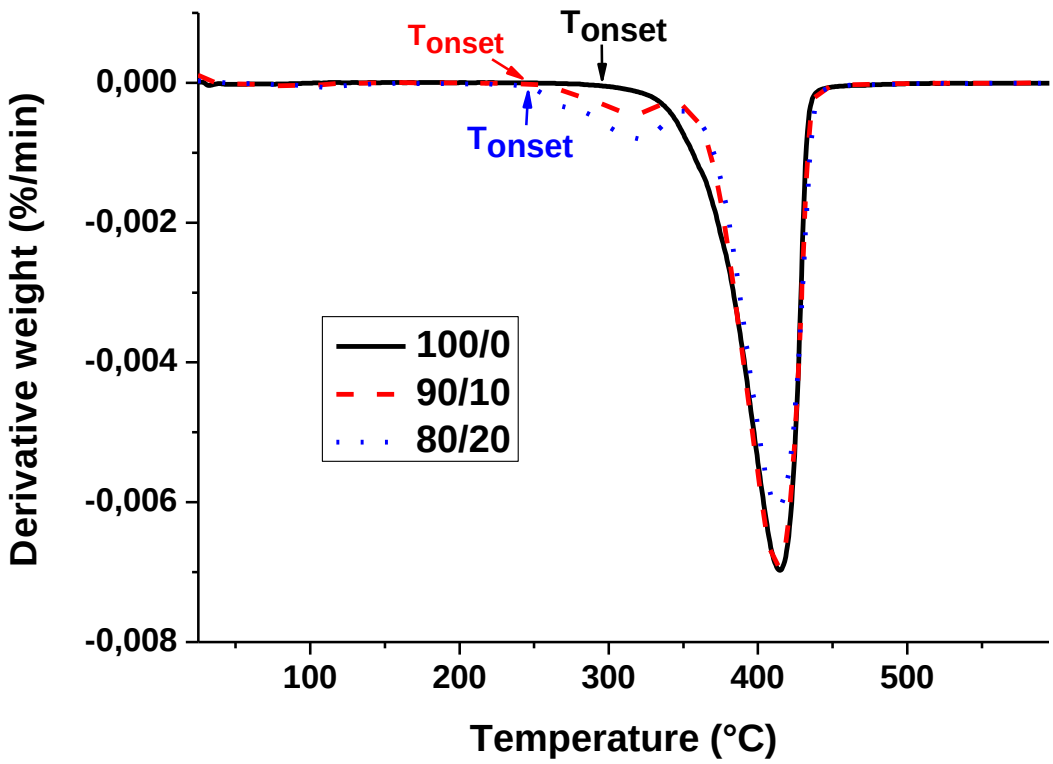

Fig 5 b. Derivative Thermogravimetric curves of PBS/CD-Lim blends: 100/0 (—), 90/10 (- - -), 80/20(…).

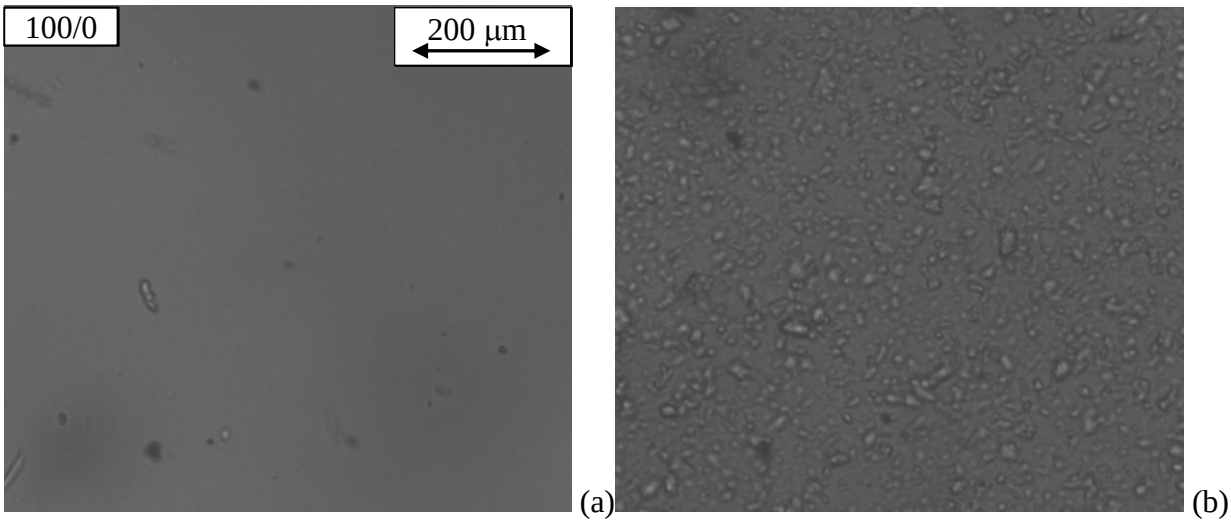

(a) (b)

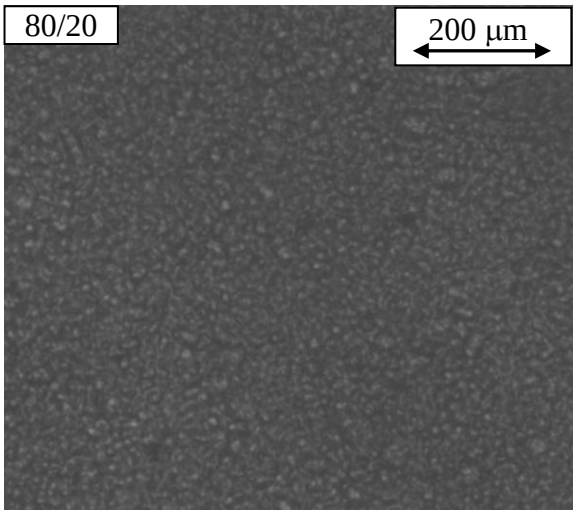

(c)

Figure 6. Optical micrographs of PBS/CD-lim composites at 135°C: (a) 100/0; (b) 90/10; (c) 80/20.

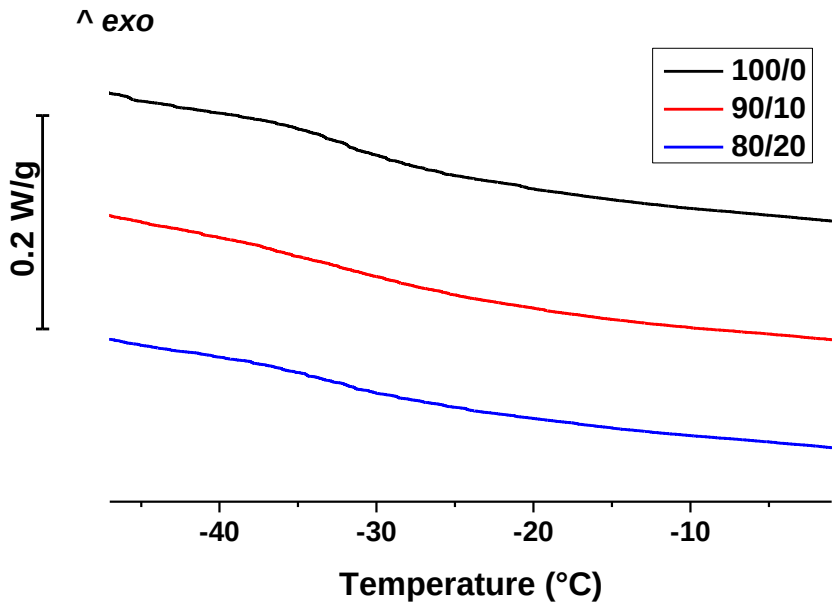

Figure 7. Glass transition temperature (T_g) of PBS based composites

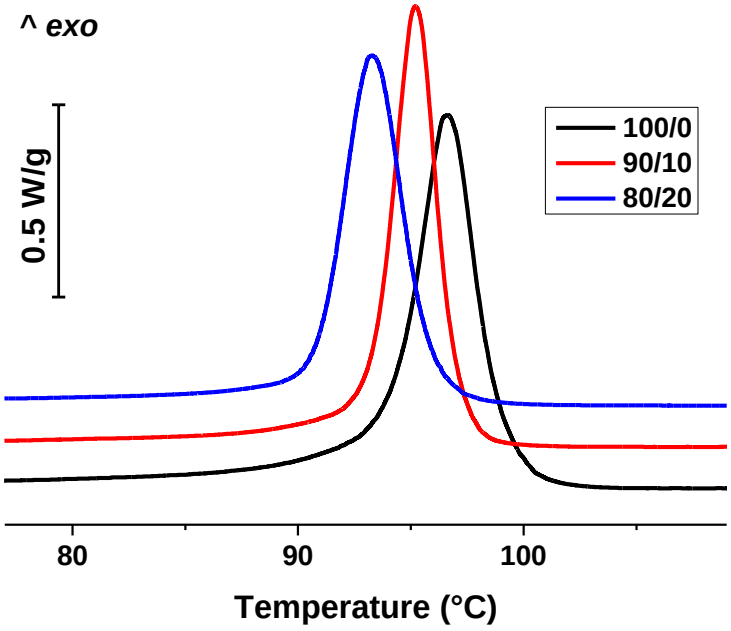

Figure 8. PBS crystallization thermograms during cooling from the melt at 4 °C/min

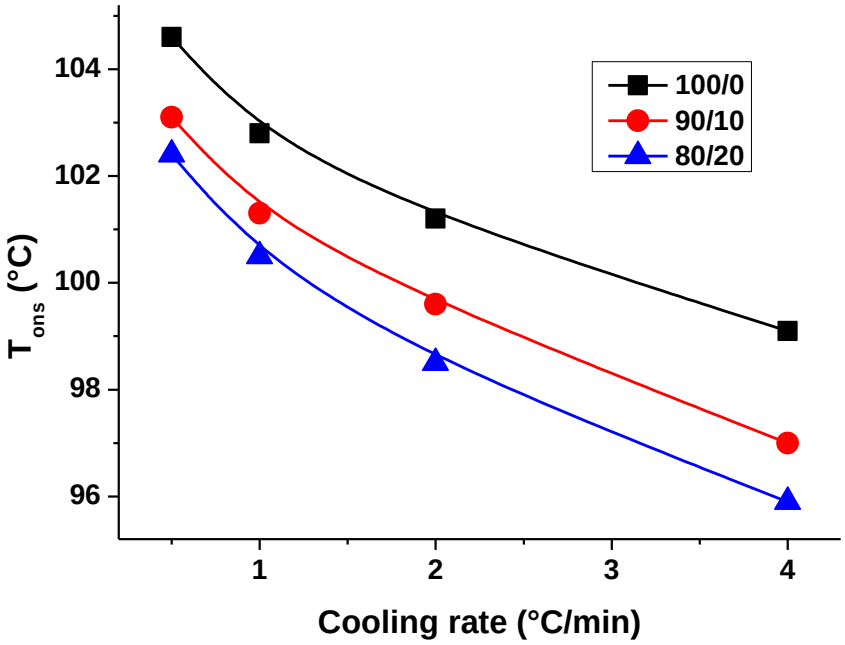

Figure 9 (a). T_{ons} of PBS crystallization exotherms as a function of cooling rate

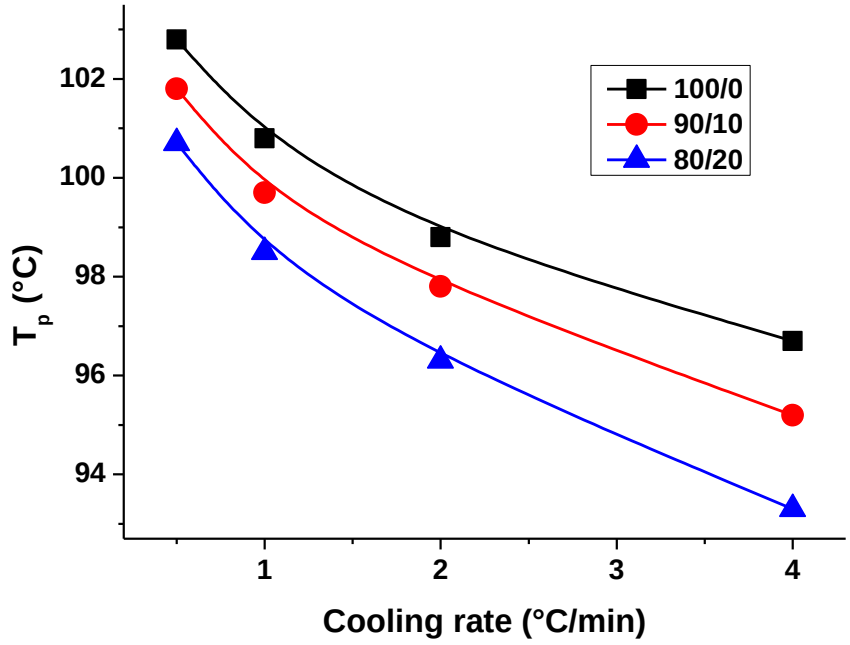

Figure 9 b T_p of PBS crystallization exotherms as a function of cooling rate

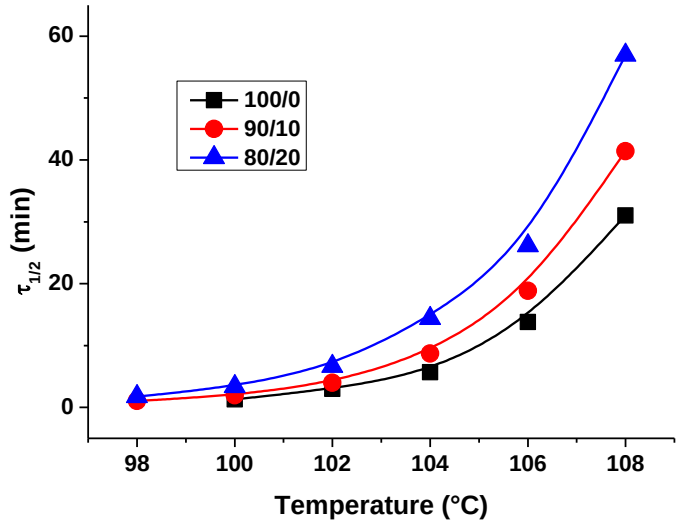

Figure 10. Half-time crystallization ($\tau_{1/2}$) of PBS exotherms as a function of temperature

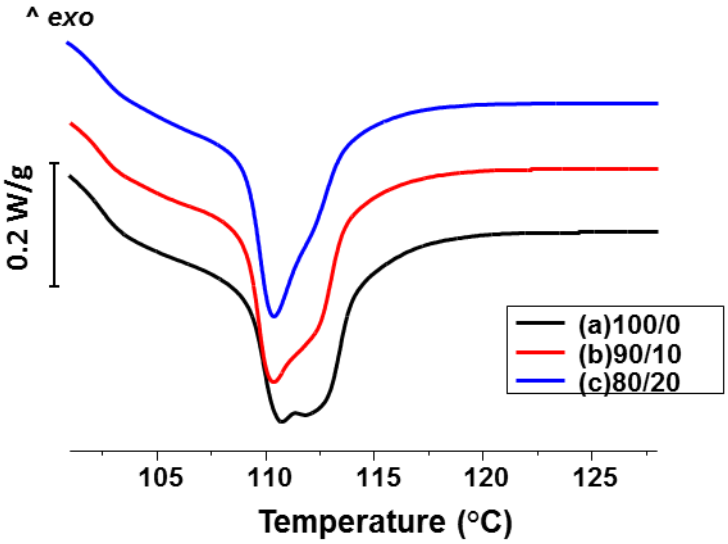

Figure 11 Melting thermograms of PBS upon heating at 20 °C/min after isothermal crystallization at 100 °C.